INSULIN SIGNALING AND SYNAPTIC PHYSIOLOGY: INSIGHTS

INTO THE PATHOGENESIS OF ALZHEIMER'S DISEASE

Except where reference is made to the work of others, the work described in this dissertation is my own or was done in collaboration with my advisory committee. This dissertation does not include proprietary or classified information.

_____
Brian Christopher Shonesy

Certificate of Approval:

_____   _____
Rajesh H. Amin   Vishnu Suppiramaniam, Chair
Assistant Professor   Associate Professor
Pharmacal Sciences   Pharmacal Sciences

_____   _____
Muralikrishnan Dhanasekaran   Robert L. Judd
Assistant Professor   Associate Professor
Pharmacal Sciences   Anatomy, Physiology and
                                                                    Pharmacology

_____   _____
Kevin W. Huggins   Forrest T. Smith
Assistant Professor   Associate Professor
Nutrition and Food Sciences   Pharmacal Sciences

_____
George T. Flowers
Dean
Graduate School

INSULIN SIGNALING AND SYNAPTIC PHYSIOLOGY: INSIGHTS

INTO THE PATHOGENESIS OF ALZHEIMER'S DISEASE

Brian Christopher Shonesy

A Dissertation

Submitted to

the Graduate Faculty of

Auburn University

in Partial Fulfillment of the

Requirements for the

Degree of

Doctor of Philosophy

Auburn, Alabama
August 10, 2009

INSULIN SIGNALING AND SYNAPTIC PHYSIOLOGY: INSIGHTS

INTO THE PATHOGENESIS OF ALZHEIMER'S DISEASE

Brian Christopher Shonesy

Signature of Author

Date of Graduation

VITA

Brian Christopher Shonesy, son of Michael and Linda Shonesy, was born on August 16, 1983, in Montgomery, Alabama. He graduated from Huntsville High School in Huntsville, Alabama in 2002. He began his research career in the laboratory of Dr. Vishnu Suppiramaniam as an undergraduate in 2005 at Auburn University, where he graduated cum laude with a Bachelor of Science degree in Biomedical Sciences on May 11, 2006. He entered the doctoral program in the Department of Pharmacal Sciences at Auburn University in 2007.

DISSERTATION ABSTRACT

INSULIN SIGNALING AND SYNAPTIC PHYSIOLOGY: INSIGHTS

INTO THE PATHOGENESIS OF ALZHEIMER'S DISEASE

Brian C. Shonesy

Doctor of Philosophy, August 10, 2009
(B.S., Auburn University, 2006)

135 Typed Pages

Directed by Vishnu Suppiramaniam

An emerging hypothesis is that desensitization of the neuronal insulin receptor (central insulin resistance) may contribute to the pathogenesis of Alzheimer's disease (AD). It is believed that deficits in glutamatergic function may underlie the cognitive deficits observed in AD. Therefore, understanding the impact of central insulin resistance on glutamatergic physiology may lead to therapeutic manipulations which halt the progression of AD before irreversible damage occurs. A useful model of central insulin resistance is the ic-STZ (intracerebroventricular streptozotocin) animal model. STZ is known to inhibit insulin receptor function in the brains of these animals. Moreover, these animals display classic AD-type pathology including amyloid-beta deposition, tau hyperphosphorylation, neuroinflammation and deficits in spatial memory performance. Therefore, these animals were utilized in this study to elucidate the effect of central insulin resistance on glutamatergic synaptic physiology.

We performed extracellular field recordings in acute hippocampal slices from ic-STZ rats and sham infused controls and found that these animals exhibit severe deficits in basal synaptic transmission and long-term potentiation (LTP). Based on input-output relations and paired-pulse facilitation experiments, we hypothesized that these deficits in synaptic transmission arise from a disturbance of postsynaptic physiology.

The AMPA-type glutamate receptor mediates the majority of basal excitatory synaptic transmission and is essential for the induction of LTP during the acquisition of new memory. Whole cell patch clamp recordings revealed a profound deficit in AMPA receptor-mediated currents, which we determined are due in part to changes in the function of the individual AMPA receptors. Protein and mRNA expression analysis from these animals suggest that these deficits may also be explained by altered AMPA receptor-subunit composition. Our results suggest that cellular trafficking of the GluR1 AMPA receptor subunit may be impaired in these brains and future investigation into the precise role of insulin in glutamate receptor trafficking seems warranted. We utilized several biochemical techniques to detect changes in GSK-3beta, Akt, integrin-linked kinase (ILK), BNDF and Erk-1/2 at the transcriptional, translational and posttranslational levels. The results of these studies suggest a novel role for ILK in synaptic plasticity and provide preliminary evidence for a role for ILK in neurodegeneration. Understanding more about this kinase and its role in neuronal function may lead to novel therapeutic targets for neurodegenerative disease and learning and memory disorders.

ACKNOWLEDGEMENTS

Style manual or journal used: Journal of Neuroscience

Computer software used: Adobe Photoshop CS2, Endnote X2, GraphPad Prism 5.0, Microsoft Excel 2008, Microsoft Word 2008, pClamp 9.0 and WinLTP

TABLE OF CONTENTS

LIST OF FIGURES

LIST OF TABLES

CHAPTER I:

INTRODUCTION

Alzheimer's disease (AD) is the most common form of dementia, affecting nearly 4.5 million Americans according to the 2000 census (Hebert et al., 2003). It is estimated that the without significant advancements in the prevention of this disease, the U.S. prevalence will reach 13 million by 2047 (Brookmeyer et al., 1998). AD is characterized by two classical pathological hallmarks, the intracellular neurofibrillary tangles and the extracellular senile plaques composed of tau protein and amyloid-β peptide respectively. Previous reports demonstrate that hippocampal synaptic dysfunction precede frank neuronal degeneration in AD (Selkoe, 2002; Walsh et al., 2002); furthermore, while these deficits are associated with Aβ pathology, the underlying mechanism remains elusive.

The prevalence of insulin resistance is reaching epidemic levels, with recent survey data indicating that 26% of all adults in the U.S. show impaired fasting glucose tolerance (Cowie et al., 2006). The brain insulin system has been a major topic of focus in neurodegeneration over the past decade. Epidemiological studies provide strong evidence that there may be a link between AD and insulin dysfunction (Leibson et al., 1997; Arvanitakis et al., 2004; Janson et al., 2004; Luchsinger et al., 2004; Kulstad et al., 2006); furthermore, recent research indicates that insulin may have a role in normal cognitive function, particularly in the hippocampus, a structure involved in memory

encoding. It is clear that learning and memory deficits are present in both type 1 and type 2 diabetes (Perlmuter et al., 1984; U'Ren et al., 1990; Gispen and Biessels, 2000), and that insulin dysfunction is associated with neurodegenerative pathology (Craft and Watson, 2004; Luchsinger et al., 2004; Watson and Craft, 2004). Moreover, insulin resistance is one of the highest risk factors for Alzheimer's disease (AD); however, the mechanistic basis by which these two diseases are linked remain unclear.

An emerging hypothesis is that Alzheimer's disease may represent a state of central insulin resistance. Alzheimer's patients show lower CSF and higher plasma insulin concentration than that of normal patients (Kulstad et al., 2006). Additionally, insulin has also been shown to enhance memory in Alzheimer's patients as well as normal individuals (Kern et al., 1999; Watson and Craft, 2003). It has been previously demonstrated that abnormalities in insulin (Hoyer, 1996; Boyt et al., 2000; Hoyer, 2004) as well as IGF signaling (Dore et al., 1997; Dore et al., 1999; Beattie et al., 2000; Jafferali et al., 2000; Costantini et al., 2006; Adlerz et al., 2007) can cause increased accumulation of amyloid-β; furthermore, correcting these abnormalities has shown much prospect for improving cognition in the aged brain (Simpson et al., 1994; Dore et al., 1997; Dore et al., 1999; Beattie et al., 2000; Jimenez Del Rio and Velez-Pardo, 2006; Xing et al., 2006; Xing et al., 2007). Insulin resistance is an underlying pathology for almost all vascular risk factors for AD. It leads directly to cardiovascular disease, hypertension, small vessel strokes and diabetes, all of which may also increase an individuals risk for developing AD.

Insulin has a profound influence on memory and cognition in the brain. It is essential for increasing glucose utilization during heightened activity, and seems to directly modulate the strengthening of synaptic connections, which occurs during memory formation. In the mammalian brain, there are several structures involved in memory function including the amygdala, neocortex, mammillary bodies and hippocampus. The hippocampus is essential for the formation of new episodic memories; furthermore, animal studies reveal that lesions, pharmacological inhibition, or genetic knockouts specific to the hippocampus result in an inability to learn as well as a loss of spatial memory (Tsien et al., 1996; Martin et al., 2002; Jacobsen et al., 2006; Pastalkova et al., 2006). Spatial memory, which is the major form of memory impaired in AD, is primarily mediated by the hippocampus. Moreover, post-mortem histopathology has demonstrated that this region is highly affected by AD pathology. Learning and memory is mediated at a cellular level through a process known as long-term potentiation (LTP) (Bliss and Lomo, 1973a), in which long lasting modifications in synaptic connections result in enhanced neuronal transmission (Bliss and Collingridge, 1993). Previous studies have shown that LTP is impaired in experimental models of Alzheimer's disease (Chapman et al., 1999; Larson et al., 1999; Walsh et al., 2002; Jacobsen et al., 2006); moreover, similar findings are found in diabetic animals (Biessels et al., 1996; Kamal et al., 2005). These findings strengthen the hypothesis that altered post-synaptic glutamatergic transmission is related to deficits in learning and plasticity in this animal model. There are two types of ionotropic glutamate receptors found at Schaffer Collateral-CA1 synapses that are responsible for the induction and maintenance of LTP,

and these are the N-methyl-d-aspartate (NMDA) receptor and the a-amino-3-hydroxy-5-methyl-4-isoxazole propionate (AMPA) receptor respectively (Muller and Lynch, 1988; Bliss and Collingridge, 1993; Dingledine et al., 1999).

There is increasing evidence that insulin signaling has important an important role in synaptic physiology (Plitzko et al., 2001; Skeberdis et al., 2001; Gerozissis, 2003; Xing et al., 2007). Insulin receptors are present at synapses, and are highly expressed in areas of rich synaptic density in the cortex and hippocampus (Werther et al., 1987), suggesting a relationship between insulin signaling and synaptic plasticity. Moreover, IR expression is upregulated in the rat hippocampus during behavioral tasks such as the Morris-Water Maze (Zhao et al., 1999). Multiple investigators have reported long lasting disturbances in learning and memory in ic-STZ animals (Mayer et al., 1990; Lannert and Hoyer, 1998; Salkovic-Petrisic et al., 2006); however, the synaptic mechanism underlying these deficits has not been examined.

The impact of central insulin resistance on glutamatergic physiology has not been previously investigated. A useful model of central insulin resistance is the ic-STZ (intracerebroventricular streptozotocin) animal model. STZ is known to inhibit insulin receptor function in the brains of these animals. More importantly, however, these animals eventually develop classic AD-type pathology including amyloid-β deposition, tau hyperphosphorylation, neuroinflammation and deficits in spatial memory performance. Therefore, these animals were utilized in this study to elucidate the effect of central insulin resistance on glutamatergic synaptic physiology. The first specific aim of this study was to establish whether or not these animals displayed deficits in long term

potentiation, which we predicted would occur based on previous reports demonstrating impairments in hippocampal-dependent memory performance in these animals. Once we established that these animals did in fact have deficits in plasticity, we then attempted to elucidate a mechanism accounting for these observations.

Synaptic deficits are the primary cause of memory impairment in AD and precede the neuronal atrophy associated with late stage AD. Therefore, a thorough understanding of the changes in synaptic physiology and the etiology of these alterations would lead to the development of therapeutic manipulations which can halt the progression of AD before irreversible damage occurs. Therefore, this study examined the changes in glutamatergic synaptic physiology at the cellular, molecular and neuronal circuit level. Elucidating the influence of central insulin resistance on synaptic transmission and synaptic plasticity in an animal model where plasma glucose remains normal is essential to fully understanding the role of insulin signaling in synaptic function. Furthermore, correlating the alterations mRNA and protein expression levels of important synaptic proteins with changes synaptic plasticity in ic-STZ animals provides a more detailed understanding of the complex mechanism by which the insulin-signaling pathway modulates synaptic physiology. The results of this study also highlight important differences between reported effects on synaptic physiology in type 1 diabetic animals and AD experimental models, which will aid in our understanding of etiology of the memory deficits observed in both of these diseases.

CHAPTER II: REVIEW

OF LITERATURE

The Hippocampus

The hippocampus is located in the medial temporal lobe of the cerebral cortex, and is one of the most widely studied structures of the brain. The relatively simple cellular organization and highly organized laminar network of its inputs has made it a popular model system amongst investigators. More importantly, the hippocampus has received a great deal of attention due to its essential role in learning and memory. The hypothesis that the hippocampus is important for the formation of new memories is supported by the evidence that damage to the hippocampus leads to anterograde amnesia, which is a deficit in storing new memories. Furthermore, the hippocampus is also believed to play a role in the long-term storage of information, as damage can also affect access to memories prior to the damage, which is called retrograde amnesia (Scoville and Milner, 1957). Older memories, however, remain intact after lesioning suggesting that over time the transfer of information out of the hippocampus and into other parts of the cortex occurs.

As shown in figure 2-1, the hippocampus is subdivided into four subregions called Cornu Ammonis (CA) areas, which are the CA4, CA3, CA2 and CA1. Just adjacent to the CA is the dentate gyrus (DG), which is divided into the fascia dentata and

the hilus. The neurons in the CA4 region do not have pyramidal morphology like those in the other CA subregions, for this reason many neuroanatomists do not recognize the CA4 as a separate region, but instead consider it as part of the hilus. The hippocampus receives neocortical input primarily through layer II of the entorhinal cortex, which projects onto granule cell dendrites of the fascia dentata via perforant pathway axons. Axons of the granule cells make up the mossy fiber pathway, which project to the hilus and CA3 region. In addition to the mossy fibers, the CA3 receives input from the contralateral hippocampus through the commissural pathway. The majority of axons from CA3 pyramidal cells make up the Schaffer collateral pathway which inputs onto pyramidal neurons of the CA1; however, some send fibers back to the hilus and others may also form recurrent connections terminating within the CA3. The small region between the CA3 and CA1 is the CA2, which receives input from layer II of the entorhinal cortex via perforant path fibers. The pyramidal cells of the CA1 send axons to layer V of the entorhinal cortex and forward to the subiculum, which closes the hippocampal-processing loop, which begins in layer II of the entorhinal cortex, and ends in layer V.

Glutamatergic Synaptic Transmission

Glutamate is the major excitatory neurotransmitter in the hippocampus as well as the entire CNS. After release from the presynaptic bouton, glutamate crosses the synaptic cleft and can activate both ionotropic (iGluRs) and metabotrobic (mGluRs) receptors. The iGluR family is composed of the α-amino-3-hydroxy-5-methyl-4-isoxazolepropionic acid (AMPA), kainite and N-methyl-D-aspartate (NMDA) receptors.

These receptors contain cation specific ion channels, which mediate the flux of sodium, potassium and calcium ions when activated by glutamate. mGluRs are G-protein coupled receptors whose activation results in the activation of an intracellular secondary messenger system.

The activation of ionotropic glutamate receptors results in an excitatory postsynaptic potential (EPSP). Fast inward current generated by AMPA receptors contributes to the early phase of the EPSP. The role of kainate receptors in synaptic transmission is poorly understood, but it is thought that they do not contribute to the fast EPSP. However, a low amplitude kainite receptor-mediated current can be detected in some neurons in response to high-frequency stimulation (Castillo et al., 1997; Cossart et al., 1998; Cossart et al., 2002). The ion channel of the NMDA receptor is blocked by a Magnesium ion at resting membrane potential. This blockade is relieved upon membrane depolarization, thus NMDA receptors are both ligand and voltage gated ionotropic receptors (Crunelli and Mayer, 1984; Mayer et al., 1984; Nowak et al., 1984).

AMPA Receptors

When an AMPAR is activated by glutamate, the rise time of the current response reflects the time required for glutamate to induce a conformational change in the receptor such that the ion channel opens allowing the flux of ionic current. The reverse of this, receptor deactivation, is reflected by the decay time and is the process by which glutamate is released from the binding domain and the ion channel closes. If the time of glutamate exposure is prolonged, the persistent reactivation of the receptor results in another time course of channel closure known as desensitization. During desensitization,

glutamate remains bound to the ligand-binding domain; however, the receptor adopts a distinct conformation, which results in channel closure. The extent to which the rates of deactivation and desensitization contribute to synaptic transmission varies according to a variety of factors including glutamate clearance from the synaptic cleft, the geometry of the synapse, and the type of synapse (Jonas, 2000).

The ionotropic glutamate receptors share a common structure. They are all multimeric assemblies consisting of four to five subunits consisting of four hydrophobic transmembrane regions within the central region of the amino acid sequence. They are unique compared to the subunits of most ionotropic receptors in that their second transmembrane region forms a reentrant loop resulting in an extracellular N-terminus and an intracellular C-terminus.

AMPA receptors are expressed as a combination of four subunits, GluR1-4, as ion channel tetramers (Rosenmund et al., 1998). The subunit composition directly influences a variety of properties of the ion channel itself as well as the localization of the receptor. Homomeric channels composed of GluR1, GluR3 and GluR4 are calcium permeable and inwardly rectifying. In contrast, homomeric GluR2 channels, although rarely expressed in non-manipulated physiological systems, are impermeable to calcium and have outwardly rectifying properties (Hollmann et al., 1991; Burnashev et al., 1992). More importantly, the properties of this subunit override the properties of any of the other subunits so that any channel containing the GluR2 subunit will be calcium impermeable and outwardly rectifying, regardless of the presence of GluR1-3 (Hollmann et al., 1991; Jonas and Burnashev, 1995). This phenomenon is due to an arginine residue in place of

glutamine in the pore-forming region of GluR2, which is the lone determinant for both calcium permeability and IV relationship (Hume et al., 1991). Even more interesting was the discovery that the arginine codon (CGG) in GluR2 is actually encoded as a glutamine codon (CAG) in the DNA sequence. Thus indicating that this difference is mediated by posttranscriptional mRNA editing (Sommer et al., 1991). This "Q/R" editing occurs in >99% of all GluR2 mRNA transcripts (Seeburg, 2002).

Another structural determinant of AMPAR properties is alternative splicing of the second extracellular region of all four GluR subunits, which is designated as "flip" and "flop" and shown in figure 2-2 (Sommer et al., 1990). Splicing of this flip flop region has a profound effect on the ligand-binding and kinetic properties of the AMPAR, and is differentially regulated according to development and anatomical location (Nakanishi, 1992). Specifically, the flop variant has a faster rate of desensitization in response to glutamate than the flip (Sommer et al., 1990).

AMPA Receptor Trafficking

The surface expression of AMPARs on the postsynaptic membrane is highly regulated has an extreme influence on synaptic excitability. Receptor surface expression is controlled at multiple levels. The first is transcriptional regulation, which is relatively poorly understood. Interestingly, Turringiano and colleagues showed that inhibition of synaptic transmission upregulates AMPAR transcription (Turrigiano et al., 1998), presumably as a means of compensation. Another means by which AMPAR density may be regulated is through trafficking. AMPA mRNA is translated on the rough endoplasmic reticulum (ER), and following translation is glycosylated at its N-terminus

while still in the ER. In the ER, the four AMPAR subunits will assemble in different combinations forming tetrameric channels (Rosenmund et al., 1998). Generally, most will contain GluR1/2 or GluR2/3 combinations; however, this varies according to developmental stage and anatomical location. Following export from the ER, AMPARs are trafficked to the Golgi, where the glycosylated N-terminus is further modified. Following this, the receptors are packaged in cytosolic vesicles and translocated to the synaptic terminal region.

The targeting and insertion of AMPARs onto the surface of the postsynaptic membrane is extremely complicated and still not completely understood. Whether or not AMPARs are first inserted at extrasynaptic sites and then laterally diffuse to synaptic locations has not been fully elucidated. However, a recent study reported that AMPARs are first inserted at somatic locations and traverse along the dendrite (Adesnik et al., 2005). Still others support a mechanism where AMPARs are trafficked via the cytoskeleton and are directly inserted into the postsynaptic density (Gerges et al., 2006). Moreover, a third possible mechanism is that AMPARs are synthesized directly in dendritic compartments and then inserted at dendritic sites (Passafaro et al., 2001).

The surface expression of AMPARs is also dependent on the subunit composition. Under basal conditions, the exocytosis of GluR1 and GluR4 receptors occurs slowly (Hayashi et al., 2000), whereas GluR2 is rapid and occurs constitutively (Passafaro et al., 2001). During heightened synaptic activity and NMDAR activation, GluR1 and GluR4 receptor insertion is enhanced and GluR1 trafficking signals dominate over GluR2 (Hayashi et al., 2000).

It was previously thought that AMPAR trafficking to the surface of the postsynaptic membrane was mediated entirely by interactions between the C-terminus of GluR2 and several cytoplasmic proteins including PICK1, GRIP1, NSF, and SAP97 (Milstein and Nicoll, 2008). However, it has since been discovered that AMPARs associate with stargazin, a four-pass transmembrane protein that directly interacts with postsynaptic density-95 (PSD-95) via a C-terminal PDZ-binding domain (Chen et al., 2000; Schnell et al., 2002; Bats et al., 2007). This transmembrane AMPAR regulatory protein (TARP) is essential for the trafficking of AMPARs to the surface of the postsynaptic membrane (Hashimoto et al., 1999; Vandenberghe et al., 2005). Moreover, studies that are more recent have reported that stargazin has a profound effect on the functional properties of AMPARs. Specifically, it has been demonstrated that stargazin slows the rate of AMPAR activation, deactivation and desensitization (Priel et al., 2005; Tomita et al., 2005; Turetsky et al., 2005; Milstein et al., 2007). Single-particle electron microscopy revealed that stargazin has an effect on the conformational structure of AMPARs (Nakagawa et al., 2005). Furthermore, this is supported by single-channel patch clamp recordings in which the TARP increases the channel conductance (Tomita et al., 2005; Soto et al., 2007).

AMPARs are phosphorylated at multiple sites along the C-terminal domain by protein kinase A (PKA), calcium calmodulin-dependent kinase II (CaMKII) and protein kinase C (PKC) (Roche et al., 1996). Phosphorylation results in the interaction between the C-terminal domain and PSD-95 as well as with GRIP, PICK, NSF and SAP97 which respectively enhance AMPAR surface expression and anchoring to the PSD (Sheng and

Lee, 2001), promote AMPAR clustering (Xia et al., 1999) and facilitate AMPAR exocytosis (Nishimune et al., 1998).

NMDA Receptors

N-methyl-D-aspartate receptors (NMDARs) are ionotropic ligand-gated voltage-dependent glutamate receptors, composed of assemblies of the NMDAR subunits NR1, NR2 and NR3 (Hollmann et al., 1989; Moriyoshi et al., 1991; Monyer et al., 1992). The NR1 subunit exists as eight splice isoforms (Dingledine et al., 1999. In heteromeric complexes NR1 is the essential subunit (Forrest et al., 1994) required for the formation of functional NMDARs; furthermore, it also contains the binding-domain for the co-agonist glycine (Monyer et al., 1992; Anson et al., 1998; Banke and Traynelis, 2003). The NR2 subunit contains the glutamate-binding domain (Planells-Cases et al., 1993) and is subdivided into the four subtypes NR2A-D each encoded by a different gene. The NR2 subunits differ in their structural and pharmacological properties and are main determinants of NMDAR function. NMDARs are composed of two NR1 subunits and either two NR2 subunits or NR3 subunits (Sheng et al., 1994; Behe et al., 1995). The NR2 subunits can either be a heteromeric tetramer of two NR1 and two NR2A subunits or two NR1 and two NR2B subunits. Triheteromeric tetrameric NMDARs also exist, for example a receptor may consist of two NR1, one NR2A and one NR2B (Dunah et al., 1998). In the hippocampus of adult mice, NMDARs are primarily composed of NR2A and NR2B heteromers, with a small portion of triheteromeric NR2A/NR2B receptors present as well. The NR2 subunits dictate the functional properties of the channels,

affecting the channel open time, conductance and magnesium sensitivity. Furthermore, the NR2 subunit expression is regulated developmentally.

The surface distribution of NMDA receptors can be classified into three catagories: synaptic, perisynaptic and extrasynaptic. The synaptic NMDA receptor pool is defined by its association with the postsynaptic density (PSD) and are activated by synaptically released glutamate. The perisynaptic pool are approximately 300 nm from the PSD (Clark and Cull-Candy, 2002; Petralia et al., 2005; Zhang and Diamond, 2006) and are still in close enough proximity to respond to synaptically released glutamate, but only during strong synaptic stimulations. Interestingly, a small portion of synaptic NMDA receptor signaling is dependent on synaptically released glutamate from adjacent synapses in hippocampal pyramidal neurons (Scimemi et al., 2004). The third pool, which is far less understood, is the extrasynaptic pool of NMDA receptors. The surface density of these receptors is far lower than that of the synaptic an perisynaptic receptor pools; however, the receptors represent about a third of the total NMDA receptor surface population in adults and nearly two-thirds in early developmental stages (Tovar and Westbrook, 1999; Groc et al., 2006). Extrasynaptic NMDA receptors are probably not activated by synaptically released glutamate under physiological conditions but may be activated by glutamate derived from other sources. Moreover, some have hypothesized that pathological conditions may exist whereby surges in synaptic glutamate release may occur in sufficient amounts to induce spillover into extrasynaptic sites, thereby activating the extrasynaptic pool of NMDA receptors (Misra et al., 2000; Clark and Cull-Candy, 2002; Brickley et al., 2003). This hypothesis is of particular relevance to Alzheimer's

disease, in which increased presynaptic glutamate release is thought to underlie the overactivation of NR2B NMDA receptors, predominate the extrasynaptic pool, leading to excitotoxicity and synaptic depression.

The predominating hypothesis concerning the subunit composition of the different pools is that surface NR2A containing receptors were primarily found in the synaptic pool with NR2B predominately located in the extrasynaptic pool (Carmignoto and Vicini, 1992; Khazipov et al., 1995; Shi et al., 1997; Kew et al., 1998; Tovar and Westbrook, 1999; Liu et al., 2004). However, this view has been recently challenged by recent reports demonstrating a more significant presence of NR2A and NR2B in the extrasynaptic and synaptic pools respectively (Luo et al., 1997; Mohrmann et al., 2002; Groc et al., 2006; Thomas et al., 2006). These variations in NMDA receptor distribution have prompted interest in the mechanism by which different receptor subunits are segregated into distinct receptor pools and into the function of each discrete pool of surface NMDA receptors in relation to synaptic plasticity.

The results of several reports suggest that the localization of NMDA receptors to the synaptic pool is regulated by NMDA receptor interaction with PDZ-binding domain proteins especially PSD-95 (Li et al., 2002; Li et al., 2003; Lim et al., 2003). Mutation-induced truncation of the PDZ-binding site where NR2B-containing receptors interact with SAP-102 and PSD-93 subunit causes complete loss of NR2B receptors in the synaptic pool (Barria and Malinow, 2002; Mohrmann et al., 2002; Prybylowski et al., 2005). Truncation of the C-terminus of the NR2A subunit reduces NMDA evoked and mEPSC-mediated currents, with no change in the extrasynaptic NMDA current (Sprengel

et al., 1998; Steigerwald et al., 2000); however, mutations which are known to prevent the interaction of NR2A with PDZ-scaffolding proteins has no effect on synaptic currents (Prybylowski et al., 2005; Thomas et al., 2006). An explanation for these contradicting results has yet to be elucidated, and further investigations are warranted.

Long-term potentiation

In *The Organization of Behavior* (1949), Donald Hebb hypothesized that the organization and activity of neurons may serve as a cellular mechanism of memory storage (Hebb, 1949). The first experiment proving the Hebbian model was conducted by Bliss and Lomo in 1973, where they coined the term long-term potentiation (LTP) (Bliss and Lomo, 1973b). The storage of information in the brain is mediated by activity-dependent changes in synaptic efficacy in a process known as synaptic plasticity (Bliss et al., 2003). Although proof that LTP is necessary and sufficient for learning and memory is lacking, several reports have demonstrated the occurrence of LTP *in vivo* following behavioral learning and memory tasks (Martin et al., 2000; Whitlock et al., 2006).

The process of LTP is composed of two phases: induction or early LTP (E-LTP) and maintenance or late LTP (L-LTP). These phase correspond to behavioral memory, which also has two components: short-term memory and long-term memory (Lynch, 2004). During LTP induction, glutamate is released from the presynaptic terminal and activates AMPARs and NMDARs on the postsynaptic terminal. Depolarization of the membrane causes the release of the NMDA-Mg^{2+} blockade, which activates NMDARs allowing influx of Na^+ and Ca^{2+} into the dendritic spine. Increasing Ca^{2+} concentration in the dendritic spine activates calcium/calmodulin-dependent protein kinase II (CaMKII)

(Malenka, 1994). Several signaling pathways are involved in LTP induction including, cAMP-dependent protein kinase (PKA) (Esteban et al., 2003), protein kinase C (PKC) (Boehm et al., 2006), extracellular signal-regulated kinase 1/2 (ERK 1/2) in the mitogen-activated protein kinase (MAPK) cascade (Atkins et al., 1998), phosphatidylinositol 3-kinase (PI3-kinase) (Opazo et al., 2003) and tyrosine kinase Src (Hayashi and Huganir, 2004). The maintenance phase of LTP is also known as the protein synthesis-dependent phase. Proteins synthesized during the maintenance of LTP include AMPAR subunits, transcriptional factors and cytoskeletal components involved in morphological enhancement of dendritic spines (Matus, 2000; Fukazawa et al., 2003).

Changes in synaptic strength is governed by the precise timing of presynaptic release in combination with the firing of an action potential in the postsynaptic membrane in a process known as spike-timing-dependent plasticity (Sjostrom and Nelson, 2002; Dan and Poo, 2004). This timing is essential for the activation of NMDARs on the postsynaptic membrane, which require both the binding of glutamate in concert with membrane depolarization (Markram et al., 1997). Calcium influx into the postsynaptic terminal is essential for the expression of both long-term potentiation (LTP) and long-term depression (LTD). It appears that the amount and kinetics of calcium influx largely determines the direction of plasticity, with large and rapid influxes contributing to LTP and smaller prolonged influxes leading to LTD (Sjostrom and Nelson, 2002). These small yet precise changes in calcium influx are primarily responsible for activating the downstream signaling events that lead to LTP and LTD. Over the past two decades, most investigators have focused their attention on several postsynaptic processes that may

17

underlie synaptic plasticity including the regulation of AMPARs (Malinow and Malenka, 2002), regulation of the actin-cytoskeleton (Matus, 2000), regulation of protein synthesis (Steward and Schuman, 2003), and regulation of gene expression (West et al., 2002).

Synaptic strength can be enhanced by increasing the number of AMPARs on the postsynaptic membrane, as well as by enhancing the functional properties of each individual receptor. Moreover, the composition of these receptors has a profound influence on synaptic efficacy. Phosphorylation of Ser831 by CaMKII and PKC or by PKA at Ser831 on the intracellular C-terminus of GluR1 significantly increases the single-channel conductance (Roche et al., 1996; Derkach et al., 1999). The phosphorylation of these sites on the calcium-permeable GluR1 AMPAR subunit has been indentified as essential for the normal expression of LTP and memory formation (Lee et al., 2003).

Insulin and the Brain

Historically, the brain was believed to be an insulin-insensitive tissue. However, this view has been recently disproved by evidence from behavioral, biochemical, cellular, and molecular studies demonstrating that insulin is present in certain regions of the CNS. Moreover, insulin has been shown to be an important neuromodulator and its dysfunction has the ability to affect pathophysiology in disease of neurodegeneration (Park, 2001; Schulingkamp, 2000; Schwartz et al., 2000; Woods et al., 2000).

Insulin Signaling Pathway

The primary function of insulin is the regulation of energy homeostasis. Insulin is able to induce a wide range of downstream signaling cascads through the activation of the insulin receptor (IR) (Saltiel and Kahn, 2001). The insulin receptor is a receptor tyrosine kinases (RTKs), as is its closely related Insulin-like Growth Hormone (IGF) receptor. The downstream effects of insulin are mediated by the activation/deactivation of various signaling pathways including the Insulin Receptor Substrates (IRS), the Src family homologs (SHC), Phosphatidylinositol 3-Kinase (PI3K), GTPases like Rac1 and various kinases including Akt, integrin-linked kinase (ILK) and GSK-3β (inactivated). Upon activation of the insulin receptor tyrosine-phosphorylated IRS is activated and is capable of binding to numerous signaling molecules the most notable of these is PI3K, which has a major role in insulin functions. Figure 2-3 illustrates an overview of the insulin signaling cascade.

Insulin Signaling and Synaptic Physiology

Pathways important in the regulation of synaptic plasticity and memory formation overlap with the insulin signaling pathway; therefore, it is not surprising that insulin signaling has profound effects on information storage and synaptic physiology. Elucidating the specific involvement of insulin signaling in these processes has been difficult, however, due to its effect on glucose and the differences between brain-derived insulin and pancreatic insulin. Parenteral administration of insulin has dramatic effects on memory performance, which complicates any investigation on the role of central insulin on synaptic plasticity. For these reasons it was initially assumed that insulin's

effect on memory was essentially through the regulation of glucose utilization in neurons. However, this position has been challenged by studies demonstrating a role for insulin in synaptic function that is independent of glucose regulation (Benedict et al., 2007; Hallschmid et al., 2007). However, insulin receptor heterozygous knockout mice have been shown to have impairments in spatial memory performance (Das et al., 2005).

MAP kinase activity is regulated in part by the insulin signaling pathway. Phosphorylation of the insulin receptor substrate (IRS) proteins Shc and Gab1 leads to the activation of Ras, a small GTP-binding protein, which activates mitogen-activated protein kinase kinase I (MEK) and p44/42-MAPK, also known as Erk1/2 (Taniguchi et al., 2006). Erk1/2 activation is also an essential mediator of long-term potentiation during memory formation (Impey et al., 1999; Adams and Sweatt, 2002). Downstream effectors of Erk1/2 include transcription factors (Platenik et al., 2000; West et al., 2001), which direct the transcription of immediate early genes (IEGs) during LTP induction, and regulators of AMPA receptor trafficking (Zhu et al., 2002). Furthermore, the activity dependent induction of LTP is associated with an increase and enlargement of the dendritic spine head (Engert and Bonhoeffer, 1999; Toni et al., 1999; Yang et al., 2008), which is dependent on BDNF-mediated Erk1/2 activation (Alonso et al., 2004). However, activation of Erk1/2 has also been shown to mediate amyloid-β toxicity, and is overactivated in the Alzheimer's brain (Khan and Alkon, 2006). Therefore, further investigation into the regulation and downstream effects of Erk1/2 are necessary to understand its value as a therapeutic target in neurological disease.

Activation of IRs and IGF-1 receptors results in downstream activation of the phosphatidylinositide 3 kinase (PI3)/Akt kinase (Akt) pathway (Johnston et al., 2003; Johnson-Farley et al., 2007), an important signaling pathway for synaptic plasticity (Sui et al., 2008). Akt inactivates glycogen synthase kinase-3β (GSK-3β) by phosphorylating it at its serine-9 residue (Cross et al., 1995). GSK-3β has essential roles in several cellular functions including proliferation, differentiation and cell adhesion (Frame and Cohen, 2001). Moreover, GSK-3β has been implicated in a variety of diseases including diabetes (Frame and Cohen, 2001), Alzheimer's disease (Anderton, 1999; Grimes and Jope, 2001; Alvarez et al., 2002; Bhat et al., 2004), schizophrenia (Beasley et al., 2001; Kozlovsky et al., 2002) and bipolar disorder (Grimes and Jope, 2001). GSK-3β has been shown to phosphorylate both the presenilin-1 and tau proteins, implicating its role in the pathophysiology of Alzheimer's disease (Hanger et al., 1992; Kirschenbaum et al., 2001; Avila, 2004).

Recently, a direct role for GSK-3β has been elucidated by Peineau and colleagues, who report that GSK-3β activation is a necessary requirement for the induction of long-term depression (LTD) (Peineau et al., 2007). Furthermore, two independent investigations have demonstrated that GSK-3β is inhibited during the induction of LTP (Hooper et al., 2007; Peineau et al., 2007). These studies report that during LTP induction, PI3K/Akt activation occurs resulting in the phosphorylation/inactivation of GSK-3β, which implicates this kinase as a critical determinant of the direction of plasticity. The proposed model for how GSK-3β influences the direction of plasticity is shown in figure 2-4. One study also reported that

GSK-3β is directly complexed with GluR1/2 AMPA receptor subunits; however, the significance of this association has not been fully elucidated (Peineau et al., 2007).

Akt and GSK-3β are regulated by PI3K and PTEN (phosphatase and tensin homolog) respectively (Jiang et al., 2005); however, the only upstream molecule that can directly regulate the activity of both Akt and GSK-3β is integrin-linked kinase (ILK) (Naska et al., 2006). ILK is a β1-integrin cytoplasmic domain binding protein (Hannigan et al., 1996). The current understanding of the ILK-GSK-3β pathway in synaptic physiology is limited to its key role in regulating dendrite formation in developing hippocampal neurons (Naska et al., 2006; Guo et al., 2007). Although the interaction between insulin signaling and integrins has been established (Wang et al., 2007), the effect of a dysfunctional insulin-signaling pathway on ILK has not been investigated.

Peroxisome Proliferator Activated Receptors

Peroxisome proliferator activated receptors (PPARs) are ligand-modulated nuclear transcription factors, with three main subtypes α, γ, and δ. Following activation, primarily by long-chain fatty acids, they associate with peroxisome proliferating response elements (PPREs) which results in the modulation of gene transcription for multiple genes. The tissue distribution, ligand specificity and downstream effectors vary with each subtype.

GW501516 is an investigational drug in phase II clinical trials for the treatment of dyslipidemia in humans. The structure of GW501516 is shown in figure 2-5. In insulin-resistant obese rhesus monkeys, GW501516 treatment resulted in increased HDL and decreased LDL-cholesterol and triglyceride levels. Additionally, this compound

22

improved insulin sensitivity and lowered fasting plasma insulin levels (Oliver et al., 2001). A recent study reports increased angiogenesis and cardiomyocyte enlargement only five hours following a single dose of GW501516 (Wagner et al., 2009).

Alzheimer's Disease

Dementia is defined as a state of cognitive decline substantial enough to interfere with a patient's daily function. The Diagnostic and Statistical Manual, 4th edition, text revision (DSM-IV-TR) requires that memory deficits greater than what would occur in normal aging must be present in addition to the impairment of one or more other cognitive facilities including attention, language, spatial orientation, and problem solving (American Psychiatric Association. and American Psychiatric Association. Task Force on DSM-IV., 2000). Alzheimer's disease (AD) is a progressive neurodegenerative disorder characterized by memory loss, particularly short-term, and impairments in other cognitive functions leading to alterations in mood, reasoning abilities, judgment and language. The major risk factor for dementia is age, and this risk increases four fold with each decade of life after the age of sixty-five (Brookmeyer et al., 1998). Most forms of AD are sporadic with the average age of onset around seventy years old and a median survival rate between five and ten years following diagnosis (Helzner et al., 2008). Around five percent of all cases are the familial autosomal-dominant form. This type is characterized by early onset in patients typically less than 50 years of age. Three gene mutations have been identified that contribute to familial AD, all of which result in abnormal production of the amyloid-β peptide, the principle component of senile plaques. These genes include mutations in the genes coding for either the amyloid precursor protein or for the proteins

23

associated with the catalytic site of the γ-secretase complex: presenilin 1 (PSEN1) and presenilin 2 (PSEN2) (Goate et al., 1991; Levy-Lahad et al., 1995; Rogaev et al., 1995; Sherrington et al., 1995; Selkoe and Podlisny, 2002).   The cellular and molecular mechanisms involved in the pathogenesis of AD remain unclear; however, there are two pathological hallmarks of Alzheimer's disease, which are the intracellular neurofibrillary tangles and the extracellular senile plaques composed of tau protein and amyloid-β peptide respectively.

Amyloid Hypothesis

The Amyloid-β peptide (Aβ) is the product of the proteolytic cleavage of the amyloid precursor protein, and is the primary constituent of senile plaques which are hallmark to AD pathology (Masters et al., 1985). Amyloid precursor protein (APP), a transmembrane glycoprotein (Kang et al., 1987), is enzymatically processed which results in the production of various peptide fragments as shown in figure 2-6 (De Strooper and Annaert, 2000). APP is first cleaved by one of two proteolytic enzymes: α-secretase in an alternative non-amyloidogenic pathway, and β-secretase (Vassar, 2004), producing the soluble extracellular fragments,   α-APP and β-APP and three transmembrane C-terminal fragments (Simons et al., 1996). Following this proteolysis, the remaining fragment can be further processed by γ-secretase to generate amyloidogenic Aβ peptides ranging from thirty-eight to forty-three residues in length (Simons et al., 1996). Ninety percent of the Aβ generated ends at residue forty ($A\beta_{40}$), with the majority of the remaining ten percent composed of the forty-two length species ($A\beta_{42}$) (Selkoe and Wolfe, 2007).

24

Insoluble $A\beta_{42}$ is markedly increased in the Alzheimer's disease brain; nonetheless, Alzheimer's patients consistently exhibit decreased levels of soluble $A\beta_{42}$ in the CSF (Andreasen and Blennow, 2002), which is thought to reflect the increased deposition and decreased clearance in the brain (Wang et al., 1999). Observations that presenilin mutations consistently result in increased production of $A\beta_{42}$ strengthen the hypothesis that $A\beta_{42}$ is the primary species responsible for the pathogenesis of AD. (Borchelt et al., 1996; Ishii et al., 1997; Wisniewski et al., 1998). $A\beta_{42}$ polymerizes more readily, which may account for the increased toxicity compared to $A\beta_{40}$ (Jarrett et al., 1993b, a; Jarrett and Lansbury, 1993; Snyder et al., 1994). At normal concentrations $A\beta$ is a soluble protein; however, in AD brains, increased concentrations of $A\beta$ leads to peptide aggregation and the formation of less soluble forms such as oligomers, protofibrils and fibrils (Bitan et al., 2003).

Tau Hypothesis

The microtubule-associated tau protein is abnormally hyperphosphorylated in the AD brain and is the main component of the paired helical filaments (PHFs), which make up the characteristic neurofibrillary tangles (NFTs) in AD pathology (Grundke-Iqbal et al., 1986b; Grundke-Iqbal et al., 1986a; Iqbal et al., 1986). The normal physiological role of tau is to promote the formation of the tubulin-microtubule assembly (Goedert et al., 1991). In contrast to the $A\beta$-composed senile plaques, which appear relatively early in the extracellular space, NFTs are intracellular and are not seen until late in the disease state (Goedert et al., 1989a). Levels of the hyperphosphorylated tau can be detected in the cytosol before accumulation into PHFs occurs (Iqbal et al., 1986).

25

There are six isoforms of tau in the adult mammalian brain (Goedert et al., 1989b). In AD, all six isoforms of tau are hyperphosphorylated at over thirty serine/threonine residues (Morishima-Kawashima et al., 1995) by several kinases including glycogen synthase kinase-3β (GSK-3β), mitogen activated protein kinase (MAPK) ERK 1/2, cyclin dependent protein kinase (cdk5), and calmodulin-dependent protein kinase-II (CamKII) (Pei et al., 2002b; Pei et al., 2002a). Tau hyperphosphorylation may result in a loss of function modification, which may further contribute to the deficits in neuronal function.

Insulin Signaling and Alzheimer's Disease

Epidemiological studies provide strong evidence that there may be a link between AD and insulin dysfunction (Leibson et al., 1997; Arvanitakis et al., 2004; Janson et al., 2004; Luchsinger et al., 2004; Kulstad et al., 2006); furthermore, recent research indicates that insulin may have a role in normal cognitive function, particularly in the hippocampus, a structure involved in memory encoding. It is clear that learning and memory deficits are present in both type 1 and type 2 diabetes (Perlmuter et al., 1984; Gispen and Biessels, 2000), and that insulin dysfunction is associated with neurodegenerative pathology (Craft and Watson, 2004; Luchsinger et al., 2004; Watson and Craft, 2004). Conversely, insulin has demonstrated memory-enhancing effects in both human and animal trials (Kern et al., 1999; Park et al., 2000). Due to its effect on circulating glucose levels, there are, however, several caveats to studying insulin's role in synaptic physiology and AD. Additionally, insulin transport across the blood brain

barrier may be impaired in AD patients, further complicating the issue (Kaiyala et al., 2000; Kulstad et al., 2006; Persidsky et al., 2006).

Insulin receptors are present at the synapses in the brain (Abbott et al., 1999) and are highly expressed in areas of rich synaptic density in the cortex and hippocampus (Werther et al., 1987), suggesting a relationship between insulin signaling and synaptic plasticity. Moreover, insulin receptor expression is upregulated in the rat hippocampus during behavioral tasks such as the Morris-Water Maze (Zhao et al., 1999). Insulin is involved in synaptic functions of memory and has been reported to influence neurotransmitter release (Bhattacharya and Saraswati, 1991; Figlewicz and Szot, 1991), as well as modulate the trafficking and expression of $GABA_A$, NMDA and AMPA receptors (Wan et al., 1997; Beattie et al., 2000; Lin et al., 2000; Kim and Han, 2005). Furthermore, Zhao et al. reported that insulin receptor surface expression is down regulated in AD brains (Zhao et al., 2008).

It has been demonstrated previously that abnormalities in insulin signaling can lead to increased concentrations of amyloid β (Hoyer, 1996; Boyt et al., 2000; Hoyer, 2004); furthermore insulin has the ability to protect cultured hippocampal neurons against Aβ cytotoxicity (Takadera et al., 1993). The exact mechanism by which insulin interacts with Aβ is unknown; however, previous reports indicate that Aβ can compete with insulin for binding to insulin receptors, consequently causing a decline in insulin-mediated signaling (Xie et al., 2002). Oligomerized forms of Aβ are the primary component of senile plaque in the intermediate stage; furthermore, these peptides have detrimental effects on the synaptic and molecular events associated with memory (Walsh

et al., 2002). In a recent study, it was demonstrated that insulin could prevent Aβ oligomerization; moreover, this same study reported that in addition to preventing the formation of oligomers, insulin was able to prevent the block of LTP induced by Aβ (Haleem et al., 2007).

Given the numerous effects of insulin on the CNS, it is not surprising that insulin dysfunction is present in AD, nor is it unexpected that insulin treatment can improve cognition in Alzheimer's patients (Simpson et al., 1994; Dore et al., 1997; Dore et al., 1999; Beattie et al., 2000; Watson and Craft, 2003; Jimenez Del Rio and Velez-Pardo, 2006; Xing et al., 2007). The potential benefit of insulin in ameliorating the pathogenesis of AD highlights the importance of stabilizing insulin signaling in the Alzheimer's brain.

Intracerebroventricular Streptozotocin Model of Central Insulin Resistance

An experimental rat model for central insulin resistance can be produced by administering intracerebroventricular streptozotocin (ic-STZ) (Plaschke and Hoyer, 1993; Duelli et al., 1994; Lannert and Hoyer, 1998; de la Monte et al., 2006; Lester-Coll et al., 2006). STZ is a nitrosurea alkylating agent that has been used intravenously for the induction of experimental type 1 diabetes. Following systemic injection, STZ is selectively cytotoxic to insulin secreting cells, mainly pancreatic beta cells. Beta cells are essentially the only type of peripheral cell expressing the glucose transporter 2 (GLUT2), which STZ requires for cell entry, thus, limiting the effect of STZ to these cells. Until recently the DNA alkylating activity of STZ was presumed to mediate the diabetogenic effect; however, more recent efforts have suggested that protein glycosylation by STZ may play an integral role (Roos et al., 1998; Konrad and Kudlow, 2002; Konrad et al.,

2002). The specific modification involves an impairment of intracellular secretory vesicle trafficking in pancreatic beta cells (Konrad and Kudlow, 2002). Moreover, other studies have demonstrated that STZ causes poly(ADP-ribosylation), which may play a role in the early effects of STZ in beta cell function (Strandell et al., 1989). Collectively these reports provide evidence for multiple biological actions of STZ, which may explain the observation that low doses of STZ causes insulin resistance by reducing IR autophosphorylation while leaving pancreatic beta cell function intact (Blondel et al., 1989a, b; Blondel and Portha, 1989; Portha et al., 1989).

Yet another effect of STZ is seen when administered in low doses intracerebroventricularly (ic). This administration of ic-STZ does not cause systemic diabetes (Nitsch and Hoyer, 1991; Duelli et al., 1994; Lannert and Hoyer, 1998), instead ic-STZ causes central insulin resistance due to alterations in the insulin receptor affinity and expression (Blokland and Jolles, 1994; Hoyer et al., 1994; Grunblatt et al., 2004; Grunblatt et al., 2006; Lester-Coll et al., 2006). Furthermore, the observed changes that result in the ic-STZ brain exhibit great similarity to abnormalities found in the Alzheimer's brain. Significant downregulation of insulin, IR, IGF-1 and IGF-1 receptor mRNA levels are present in both the ic-STZ brain as well as the AD brain (Lester-Coll et al., 2006). Alterations in brain glucose metabolism, inflammation and oxidative stress are among the more extensively investigated properties in the ic-STZ. Additionally, previous work has shown that accumulation of amyloid-β and hyperphosphorylated tau proteins is correlated with central insulin resistance in these animals (Salkovic-Petrisic et al., 2006; Grunblatt et al., 2007; Planel et al., 2007; Salkovic-Petrisic and Hoyer, 2007).

29

Another remarkable finding is that these animals express an upregulation of the amyloid precursor protein (APP) gene, which also occurs in sporadic AD (Lester-Coll et al., 2006). Together these studies suggest that central insulin resistance, which is known to be present in ic-STZ animals and AD patients, may precipitate AD pathogenesis (Grunblatt et al., 2004; Rivera et al., 2005; Steen et al., 2005).

Multiple investigators have reported long lasting disturbances in learning and memory in ic-STZ animals (Mayer et al., 1990; Lannert and Hoyer, 1998; Salkovic-Petrisic et al., 2006); however, glutamatergic synaptic transmission and synaptic plasticity has not been previously investigated in the ic-STZ animal model.

Figure 2-1. Anatomy of the hippocampus. (Neves et al., 2008). The hippocampus is subdivided into four subregions called Cornu Ammonis (CA) areas, which are the CA4, CA3, CA2 and CA1. Just adjacent to the CA is the dentate gyrus (DG), which is divided into the fascia dentata and the hilus. The neurons in the CA4 region do not have pyramidal morphology like those in the other CA subregions, for this reason many neuroanatomists do not recognize the CA4 as a separate region, but instead consider it as part of the hilus. The hippocampus receives neocortical input primarily through layer II of the entorhinal cortex, which projects onto granule cell dendrites of the fascia dentata via perforant pathway axons. Axons of the granule cells make up the mossy fiber pathway, which project to the hilus and CA3 region. In addition to the mossy fibers, the CA3 receives input from the contralateral hippocampus through the commissural pathway. The majority of axons from CA3 pyramidal cells make up the Schaffer collateral pathway which inputs onto pyramidal neurons of the CA1; however, some send fibers back to the hilus and others may also form recurrent connections terminating within the CA3. The small region between the CA3 and CA1 is the CA2, which receives input from layer II of the entorhinal cortex via perforant path fibers. The pyramidal cells of the CA1 send axons to layer V of the entorhinal cortex and forward to the subiculum, which closes the hippocampal-processing loop, which begins in layer II of the entorhinal cortex, and ends in layer V.
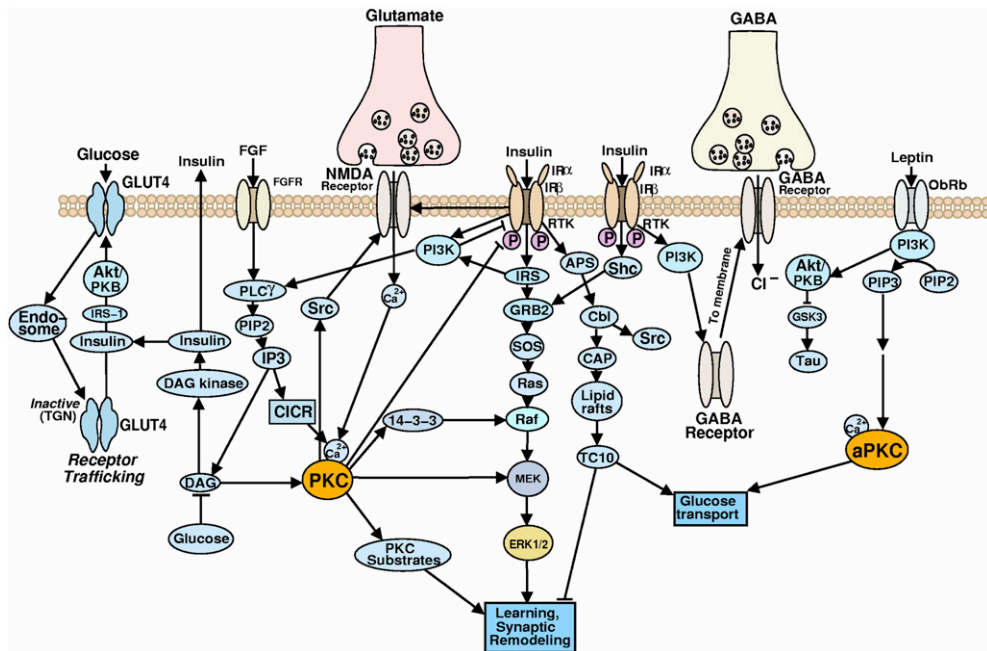
Figure 2-1.

Hippocampus
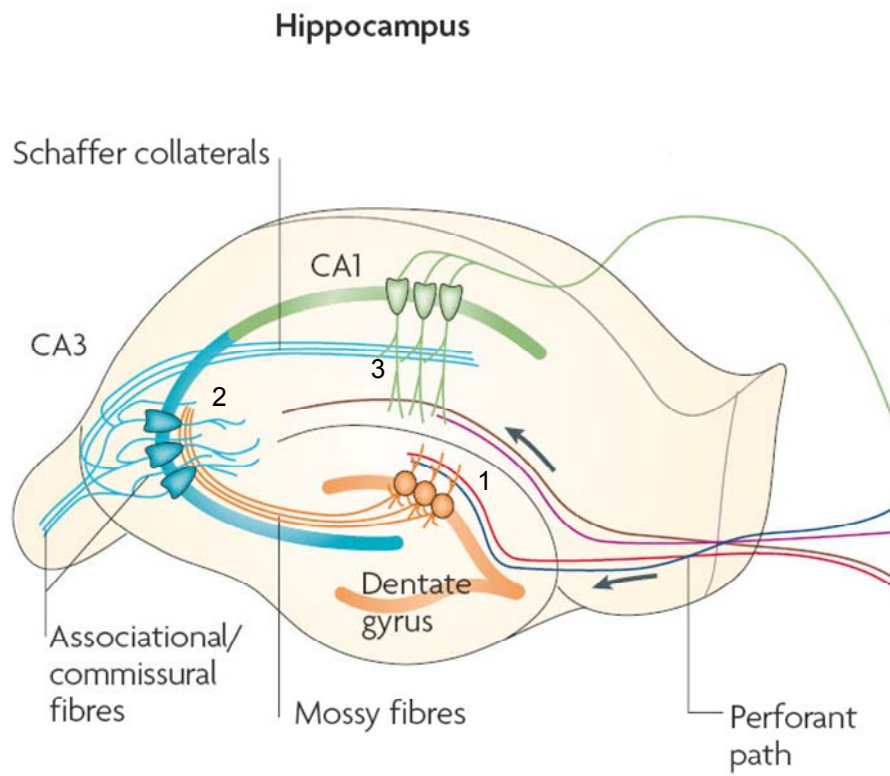
Figure 2-2. General Structure of an AMPA Receptor Subunit. The extracellular N-terminus and intracellular C-terminus is unique for transmembrane proteins. Alternative splicing of the second extracellular domain can occur and is designated as either "flip" or "flop." These variations in splicing have a profound effect on the ligand-binding and kinetic properties of the AMPA receptor. Additionally, Q/R site editing occurs in nearly all GluR2 mRNA transcripts, which underlies the altered calcium permeability of this subunit.

Figure 2-2.
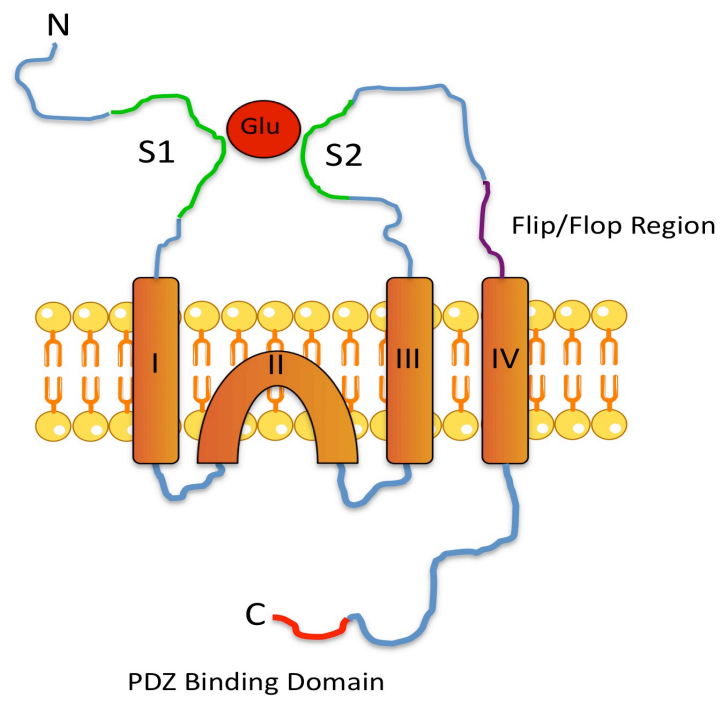
Figure 2-3. Insulin signaling pathway (Nelson et al., 2008). The downstream effects of insulin are mediated by the activation/deactivation of various signaling pathways including the Insulin Receptor Substrates (IRS), the Src family homologs (SHC), Phosphatidylinositol 3-Kinase (PI3K), GTPases like Rac1 and various kinases including Akt, integrin-linked kinase (ILK) and GSK-3β (inactivated). Upon activation of the insulin receptor tyrosine-phosphorylated IRS is activated and is capable of binding to numerous signaling molecules the most notable of these is PI3K, which has a major role in insulin functions.
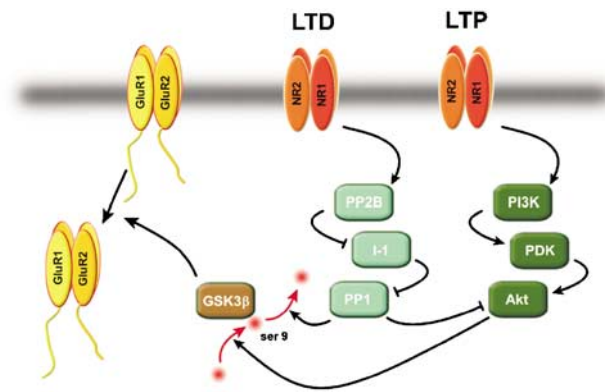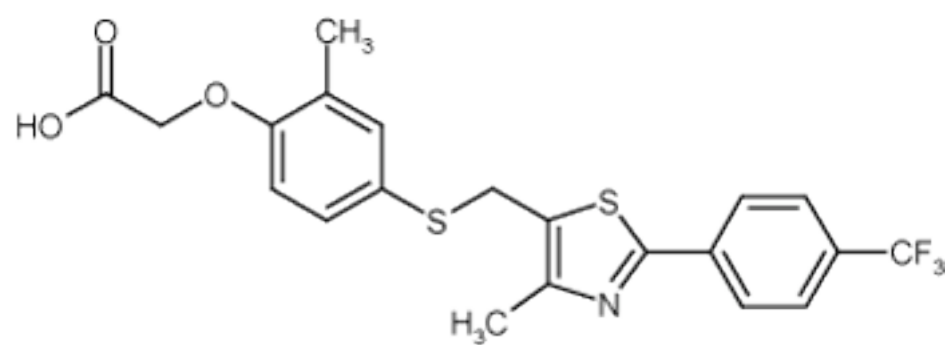
Figure 2-3.

Figure 2-4. Possible mechanism for the role of GSK-3β in synaptic plasticity (Peineau et al., 2008).

Figure 2-4.

Figure 2-5. Chemical structure of GW501516

Figure 2-5.

Figure 2-6. Amyloid Precursor Protein (APP) Processing. APP matures through the central secretory pathway, and both during and after its trafficking through this pathway. APP can undergo proteolysis by α-secretase cleavage in an alternative non-amyloidogenic pathway generating the soluble ectodomain fragment sAPPα and a membrane-retained C-terminal fragment of 83 amino acids. APP may also undergo β-secretase cleavage resulting in the release of a soluble APPβ ectodomain fragment. Following β-secretase cleavage, γ-secretase cleavage of the β-C-terminal fragment results in the production of either the forty or forty-two length Aβ peptide ($A\beta_{40}$ and $A\beta_{42}$).

Figure 2-6.
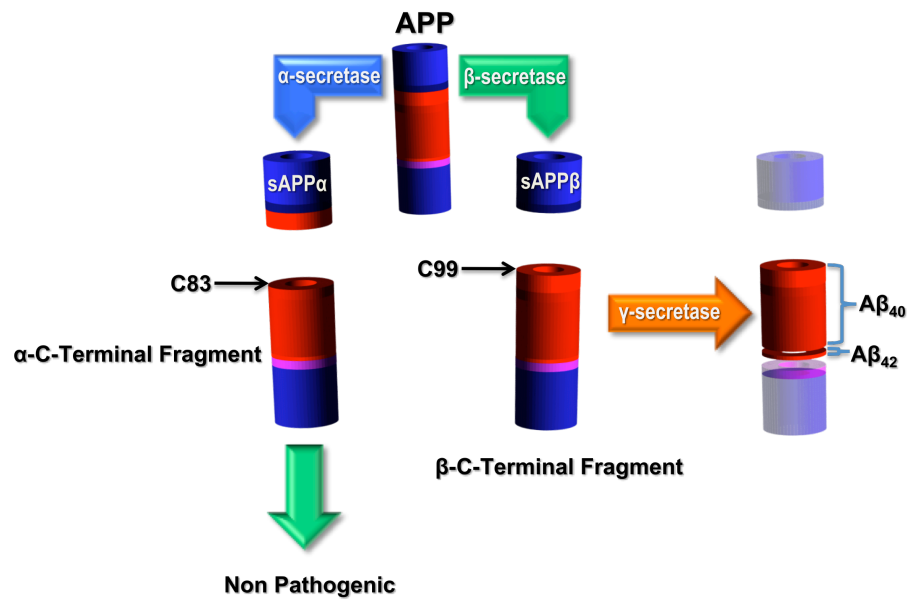
CHAPTER III:

METHODS

Animals

All procedures were approved by Auburn University Animal Care and Use Committee. Male Wistar rats (Charles River Laboratories, Wilmington, MA) were acquired at 12 weeks of age and randomly divided into 2 groups. The control group (C) received bilateral intracerebroventricular (ic) injections of 8μl per animal of artificial cerebrospinal fluid per ventricle (aCSF). The composition of aCSF was (mM) NaCl 119, KCl 2.5, $MgSO_4$ 1.3, $CaCl_2$ 2.5, NaH_2PO_4 1.0 and NaHCO3 26. The ic-STZ group (ic-STZ) received bilateral ic injections of 8μl per animal of Streptozotocin (STZ) (3mg/kg) dissolved in aCSF.

In a separate set of experiments, four control and eight ic-STZ animals were randomly selected. Four of the eight ic-STZ animals were given a single intraperitoneal (IP) injection of GW501516 dissolved in 2 ml of 20% PEG-300. The dose of 10 mg/kg was selected based on previously reported pharmacokinetic properties of this compound (Iwashita et al., 2006). The remaining four ic-STZ animals along with four control animals administered an equal volume IP sham injection of 20% PEG-300. Following administration of drug or vehicle, the animal was then placed back into its home cage for

43

three hours. After this three-hour period, the animal was anesthetized with CO_2, decapitated and hippocampal slices were prepared from the brain as described below.

Surgical Procedure

Anesthesia was induced using 4-5% isoflurane delivered through a closed circuit system with an oxygen flowrate of 1.0-1.5 L/min. Following the conformation of the appropriate plane of anesthesia, the head was then fixed in a stereotactic guidance apparatus, and anesthesia maintained using 2-3% isoflurane delivered through a nose cone. Bilateral burr holes were made in 1.0 mm posterior to the coronal suture, and 1.6 mm lateral to the sagital suture. A 30-gauge needle was lowered 3.4 mm below the Dura into the left and right lateral ventricle using stereotactic guidance. STZ (3 mg/kg) or sham aCSF was infused over a period of 3 min per ventricle in a total volume of 4 µl per ventricle.

Hippocampal Slice Preparation

A Male Wistar rat aged 16 weeks was placed in a closed chamber into which CO_2 was slowly released via until the animal reached an anesthetic state, after which it was quickly decapitated using a guillotine. A midline incision was made into the top of the head and the skin was pulled back to expose the skull. Following this, the skull was cut down the sagital suture with small iris scissors and was peeled back using a pair of bone rongeurs. The brain was quickly removed by placing a small spatula under the frontal lobe and elevating the brain away from the base of the skull. The brain was then placed into a small beaker filled with dissection buffer consisting of (in mM): NaCl 85, KCl 2.5,

MgSO$_4$ 4.0, CaCl$_2$ 0.5, NaH$_2$PO$_4$ 1.25, NaHCO$_3$ 25, glucose 25, sucrose 75, kynurenic acid 2.0, ascorbate 0.5, saturated with 95% O2/5% CO2 at a temperature of 0°C. Time for this step was minimized to 1-1.5 minutes. The cerebellum was dissected away and the brain was placed to the vibratome chamber filled with ice-cold dissection buffer bubbled with 95%O$_2$ 5%CO$_2$. The brain was held in place with cyanoacrylate glue, and was placed with the frontal lobe facing up and the basal aspect of the brain resting against a block of 10% agar. The brain was then cut into hemispheres and the two hemispheres were simultaneously cut into coronal slices of 400 μm thickness. These slices were then placed in a slice incubation chamber for thirty minutes at 30°C in artificial cerebrospinal fluid (aCSF) of the following composition (mM): NaCl 119, KCl 2.5, MgSO$_4$ 1.3, CaCl$_2$ 2.5, NaH$_2$PO$_4$ 1.0, NaHCO$_3$ 26, dextrose 11.0 and saturated with 95% O$_2$ and 5%CO$_2$. After thirty minutes, they were transferred to aCSF with a temperature of 24°C where they remained for at least another thirty minutes before being used for electrophysiological recordings.

The slice incubation chamber consisted of a round plastic vessel (7 cm in diameter and 6 cm in height) placed inside a glass crystallizing dish (10 cm in diameter and 8 cm in height). The slices were placed at the bottom of the cylinder that which was made of nylon stockings stretched and glued across the edges of the plastic vessel. The dish was filled with aCSF, and an aquarium stone was placed at the bottom of the vessel to provide the 95% O$_2$ and 5%CO$_2$.

Extracellular Field Recordings

A slice with containing an anterior portion of the hippocampus was transferred to a submersion recording chamber using a paintbrush. The recording chamber was continuously superfused at 2 ml per minute with aCSF saturated with 95%O_2 and 5% CO_2. A ring with silk strings stretched across was placed on top of the slice in such a way that the mesh did not touch the hippocampus. Healthy slices of good do not normally stick to the paintbrush and have a clearly visible stratum pyramidal and stratum granulosum. Recordings in CA3-CA1 synapses were performed by placing the stimulating and recording electrodes on surface of the slice approximately 400 µm apart from each other in the stratum radiatum where the Shaffer collateral fibers are located. All recordings were performed at 24°C. Field excitatory postsynaptic potentials (fEPSPs) were recorded from the CA1 with a glass electrode with a resistance of 1-4 MΩ filled with aCSF. Test pulses were delivered by a constant current stimulus isolator driven by input signals from the computer. The stimulus electrode was a platinum bipolar electrode. Stimulation (50-70 µA, 0.2 ms duration) was applied to CA3 axons every 20 seconds and the recording and stimulation electrodes were slowly advanced towards the slice until a the maximal amplitude of responses was attained. After ten to fifteen minutes of stable responses, the stimulus-response relation was recorded in response to stimulation pulses (0.2 ms, every 20 s) of increasing intensity by varying stimulus intensity between 0 µA to 200 µA in steps of 50 µA and measuring the slope of the fEPSPs as well as the fiber volley. Field EPSPs were recorded until a population spike (upward going inflection) appeared on the decaying phase of fEPSPs. Typically, the

amplitude of supramaximal fEPSPs was greater than one mV and the amplitude of presynaptic volleys were less than one third that of the fEPSPs.

Field EPSPs were elicited every twenty seconds for at least ten minutes with the stimulus intensity that elicited fEPSPs with a slope of 40% of the supramaximal. Obtaining stable responses of fEPSPs during the baseline period is of upmost importance to insure that the correct stimulus intensity is used. Following stable baseline recordings of at least ten minutes, a high frequency stimulus (HFS) was applied using the test pulse stimulus intensity. The HFS protocol for inducing LTP consisted of three trains of 100 pulses (100 Hz), with an inter-train interval of 20 seconds. LTP was measured as the percentage of the baseline fEPSP slope. During the 20 minute baseline and 1 hour following the tetanus, fEPSP peak amplitude and slope were analyzed online using WinLTP acquisition software (Anderson and Collingridge, 2007). The data is presented as mean ± SEM. Significance was determine using a two-tailed Student's t-test.

Paired-pulse facilitation (PPF) was evaluated by stimulating the synapses with twin pulses at interpulse intervals of 40, 60, 80, 150, and 200 ms. fEPSPs, were recorded at 40% of maximal response, as determined from an input–output curve for each experiment. Following stable baseline recordings of at least 20 minutes, a high frequency stimulus (HFS) was applied using the test pulse stimulus intensity. The HFS protocol for inducing LTP consisted of three trains of 100 pulses (100 Hz), with an inter-train interval of 20 seconds. LTP was measured as the percentage of the baseline fEPSP slope. During the 20 minute baseline and 1 hour following the tetanus, fEPSP peak amplitude and slope

were analyzed online using WinLTP acquisition software (Anderson and Collingridge, 2007).

It is important to compare baseline fEPSPs to responses after induction of LTP. If the slice is healthy and recording conditions are ideal the stimulus artifact and the amplitude of presynaptic volley should be identical prior to the application of the high-frequency stimulation and at the end of the recording. It is important to select appropriate parameters for slope measurements so that linear changes in the slope of the fEPSPs would be detectable for all stimulation intensities used to estimate the stimulus-response curve. In addition to the plot of stimulus intensity versus fEPSP slope, the presynaptic fiber volley is plotted as a function of stimulus intensity and of fEPSP slope. This function provides analysis of the number of activated axons (presynaptic volleys) and resulting fEPSPs. It is important to keep recording and stimulating electrode at a consistent and sufficiently long distance, as the presynaptic fiber volley amplitude is directly proportional to this distance. The mean magnitude of fEPSPs recorded during the baseline (at least 10 min before TBS) is taken as 100 % and changes are expressed relative to this as a means of normalizing the responses amongst multiple recordings from multiple slices. The values of LTP are calculated as the relative increase in the mean slopes of averaged fEPSPs measured at 50-60 minutes after induction of LTP. The data is presented as mean ± SEM. Significance was determine using a two-tailed Student's t-test.

Whole Cell Patch Clamp Recordings

After at least a one hour recovery period the slices were transferred to a submersion chamber where they were continuously superfused (~2 ml/min) with aCSF (24°C) saturated with 95% O_2 and 5% CO_2. Slices were visualized with Nomarski differential interference contrast optics with an Olympus BX51-WI upright microscope (Olympus, USA) equipped with a 40X water immersion objective lens. AMPA receptor mediated, action potential independent, mEPSCs were isolated from CA1 pyramidal neurons in the presence of 1 mM tetrodotoxin (TTX), 50 mM aminophosphonopentanoic acid (APV) and 30 mM bicuculline methiodide (BMI) using the whole-cell voltage-clamp technique.

Patch pipettes (1-5 MΩ) were pulled from borosilicate capillaries (nonfilamented, 1.5 mm O.D.; World Precision Instruments, Sarasota, FL) on a Sutter P-2000 Puller (Sutter Instruments, Novato, CA). The pipette was filled with a solution containing (in mM): 122.5 Cs-gluconate, 10 HEPES, 1.0 EGTA, 20 KCl, 2.0 $MgCl_2$, 2.0 $Na_2 \cdot ATP$, 2 QX-314, 0.25 $Na_3 \cdot GTP \cdot 3H_2O$, pH 7.3 (adjusted with KOH), 280–290 mOsm. GTP was included in the pipette solution to conserve G-protein mediated responses and ATP was added to prevent rundown of calcium channels and supply energy for other intracellular phosphorylation reactions. Cs^+ was included to eliminate K^+ currents.

The neurons were voltage-clamped (V_h=-70 mV) in continuous mode (cSEVC) using an Axopatch 200B amplifier (Axon Instruments Inc., Foster City, CA). Current output was low-pass filtered (10 kHz), DC-offset and amplified 10000-fold. The signal was continuously acquired on-line (Clampfit 9 Software, Axon Instruments Inc.), and

digitized (Digidata 1200, Axon). Baseline mEPSC activity was recorded in each neuron for at least 5 min. Recorded events $\geq$ 3 pA, with faster rise than decay were detected using pClamp analysis software (Molecular Devices, Sunnyvale, CA). Peak mEPSC and sEPSC amplitudes were measured from the baseline. Decay kinetics, mEPSCs and sEPSCs amplitude were also estimated using a single exponential function. Data were compared statistically by either the Student's t-test, or the Kolmogorov-Smirnov test. Results are presented as mean $\pm$ S.D.

Synaptoneurosome Preparation

Isolation of synaptosomes was carried out as described in (Johnson et al., 1997) with some modifications. Male Wistar rats 16 weeks old (4 weeks following ic-STZ or sham administration) were anesthetized with CO_2, the brains were removed and placed in ice cold aCSF. The hippocampi were isolated and homogenized (10 strokes) in a potter homogenizer and in ice cold modified Krebs-Henseleit buffer (mKRBS) containing (in mM): NaCl 118.5, KCl 4.7, $MgSO_4$ 1.18, $CaCl_2$ 2.5, KH_2PO_4 1.18, $NaHCO_3$ 24.9, dextrose 10, adenosine deaminase 10 mg/ml; pH adjusted to 7.4 by bubbling with 95% O2: 5% CO2. Protease inhibitors, leupeptin (0.01 mg/ml), pepstatin A (0.005 mg/ml), aprotinin (0.1 mg/ml) and benzamide (5 mM) were included in the buffer to minimize proteolysis. Then the homogenate was diluted with 500 ml of additional ice-cold mKRBS buffer. This mixture was loaded in a 1 cc syringe and was forced through a 100 mm pore cell strainer (BD Falcon, Bedford, MA) pre-wetted with 150 ml of mKRBS, and collected in an eppendorf tube. This filtered mixture was loaded into another 1 cc syringe and filtered through a pre-wetted 5 mm pore low protein-binding filter (Millex-SV;

50

Millipore Corp., Bedford, MA). The homogenate was kept in ice-cold temperatures during the entire procedure to minimize proteolysis. Synaptoneurosomes were then obtained through microcentrifugation at 1000 x g for 15 minutes at 48°C. The supernatant was removed and the pellets rich in synaptosomes were resuspended in 50 μl of mKRBS and stored at -80°C.

Single channel recording of synaptic AMPA receptors

Isolation of synaptosomes was carried out as previously described. The procedure for recording single channel AMPA receptor currents from synaptosomes has been described previously (Vaithianathan et al., 2005). Synaptosomal AMPA receptors were incorporated into artificial lipid bilayers using tip–dip method (Coronado and Latorre, 1983). A quartz patch pipette with a resistance of 100 MΩ was pulled using a Sutter P-2000 laser puller in a four line program with a decreasing heat and velocity on each successive line. The pipette solution contained pseudo-intracellular composed of (in mM): KCl 110.0, NaCl 4.0, NaHCO$_3$ 2.0, CaCl$_2$ 0.1, MgCl 1.0, and 3-N-morpholino propane sulfonic acid 2.0 with pH adjusted to 7.4. The 300 μl beaker contained the pseudo-extracellular solution composed of (in mM): NaCl 125.0, KCl 5.0, NaH$_2$PO$_4$ 1.25, Tris–HCl 5.0, and pH adjusted to 7.4. The synthetic phospholipids, 1,2-diphytanoyl-sn-glycero-3-phosphocholine (Avanti Polar-Lipids, Alabaster, Alabama) required for bilayer formation was prepared by dissolving in anhydrous hexane (Sigma-Aldrich, Milwaukee, Wisconson) at a concentration of one mg/ml. 5 μl of this preparation was added to the 300 μl beaker containing the pseudo-extracellular fluid. The bilayer was then formed by the successive transfer of two monolayers. Following

51

the formation of a stable bilayer membrane, monitored by a oscilloscope, 2 µl of the previously prepared synaptosomal suspension was added to the extracellular solution and gentle stirring with a magnetic microstir bar resulted in fusion of synaptosomal fragments to the lipid bilayer. The tip-dip procedure and fusion of the synaptosome is illustrated in figure 3-1. To isolate AMPA receptor single channel currents, a combination of blockers was included in the pseudo-extracellular fluid. This cocktail contained tetrodotoxin (1 µM), tetraethyammonium chloride (2 µM), APV (50 µM), methyl glutamate analog (2S, 4R)-4-methylglutamate (SYM 2081; 1 µM), and PTX (100 µM) to inhibit sodium channels, potassium channels, NMDA receptors, kainate receptors, $GABA_A$ receptors and glycine receptors respectively. AMPA receptor single channel currents were evoked by adding previously optimized, sub-maximal concentration of AMPA (290 nM) (Vaithianathan et al., 2005). At the end of all experiments, the specific AMPA receptor antagonist SYM 2206 (1 µM) was added to confirm the single channel currents recorded were AMPA receptor currents. Only experiments in which single channel currents were completely blocked by SYM 2206 were used for analysis.

Single channel AMPA currents were amplified by a Warner PC-501A Patch Clamp Amplifier (Warner Instruments, Hamden, Connecticut) and digitized by a Digidata 1200 (Molecular Devices, Sunnyvale, California) at a sampling rate of 20 kHz. The currents were low bypass filtered at 2 kHz and acquired by Clampex 9.0 (Molecular Devices, Sunnyvale, California). Offline analysis was performed using Clampfit 9.0 (Molecular Devices, Sunnyvale, California). Patches exhibiting single channel current transitions in long stretches of data were used for analysis. All-points current amplitude

histograms were constructed and fitted with a Gaussian distribution to identify the multi-subconductance levels characteristic of AMPA receptors. Single channel conductances were obtained by plotting AMPA receptor currents as a function of membrane voltage using the equation $g = I / (V-V_0)$, where g is the single channel conductance, I is the single channel current, V is the voltage and V_0 is the reversal potential. The single channel open and closed probabilities were obtained from the respective areas under the curve of the amplitude histogram.

If single channel behavior is assumed to be Markovian, the closed dwell time distributions, also referred to as the probability density function (*pdf*), can be described by a sum of several exponential functions. A channel with N_c closed states has a closed time $pdf = A_{1c}{}^{\wedge}(-t/\tau_{1c}) + A_{2c}{}^{\wedge}(-t/\tau_{2o}) + \ldots + A_{no}{}^{\wedge}(-t/\tau_{no})$, where τ_{1o}, τ_{2o}, $\ldots$, τ_{no} are the time constants and A_{1o}, A_{2o}, $\ldots$, A_{no} are the corresponding weights defining occurrence frequencies of the open states.

Gene Expression

Total RNA was isolated from 50-100 mg of whole hippocampal lysates, with on-column DNase digestion, using an RNeasy Tissue Mini Kit (Qiagen, Valencia, CA) according to the manufacturer's protocol. RNA concentration was determined by absorption spectrophotometry at 260 nm. cDNA was synthesized according to the manufacturer's protocol from 1 μg of RNA using an iScript cDNA synthesis kit (Bio Rad, Hercules, CA). Real-time PCR was performed in triplicate with 25 μl of reaction mixture in MicroAmp optical 96-well reaction plates on an iCycler real-time PCR detection instrument (Bio-Rad) using 0.5 μl cDNA, 3.0 μl 1.25 μM (final concentration)

primer mix, 9 ml RNAase free water and 12.5 µl iQ SYBR Green Supermix (Bio-Rad) per reaction. Rat gene specific primers were selected and synthesized by Integrated DNA Technologies (IDT, Coralville, IA). Primer sequences for the genes can be found in Table 1-1. The following PCR amplification cycle (40X) was used: 95° C, 180 sec; 95° C, 15 sec; 60° C, 30 sec; 72° C, 30 sec. Melt curve analysis was performed to determine specificity of products formed. Relative gene expression was determined by the comparative C_T method (Pfaffl, 2001). Gene expression was normalized to β-actin for each experimental gene tested. The data is presented as mean ± SEM. Significance was determined using a two-tailed Student's t-test.

Protein Extraction and Western Immunoblot

Whole hippocampal homogenates or synaptoneurosomes were lysed in a chilled buffer containing protease and phosphatase inhibitors (50 mM Tris-HCl, pH 7.4, 1% NP-40, 0.25% Na-deoxycholate, 150 mM NaCl, 1 mM EDTA, 1 mM PMSF, 1 µg/ml each aprotinin, leupeptin, and pepstatin, 1 mM Na_3VO_4, and 1 mM NaF). The lysates were incubated for 15 min on ice and centrifuged for 15 min at 10,000 x g, at 4°C. The supernatants containing the protein extract were collected, and their protein concentration was determined by the BCA protein assay (Pierce, Rockford, IL). Duplicate samples for individual rats were subjected to 10% SDS-PAGE and subsequently blotted to polyvinylidene difluoride membranes (Immobilon-P; Millipore, Bedford, MA). The membranes were saturated with 5% non-fat dry milk (Biorad) or 1% BSA and then incubated with anti-Akt (1:1000; Cell Signaling Technology), anti-phospho-Akt (1:1000; Cell Signaling Technology), anti-ILK (1:1000; Cell Signaling Technology), anti-GluR1

54

(1:1000; Millipore), anti-GluR2 (1:1000; Millipore), anti-NR1 (1:1000; Millipore), anti-NR2A (1:2000; Santa Cruz), anti-NR2B (1:500; Santa Cruz), anti-BDNF (1:500; Millipore), anti-stargazin (1:1000; Cell Signaling Technology), anti-p44/42, anti-phospho-p44/42 (1:1000; Cell Signaling Technology) or anti-GAPDH (1:5000; Millipore) antibodies overnight at 4°C. The membranes were subsequently incubated at room temperature for 1 hour with the corresponding anti-rabbit or anti-mouse antibodies (1:5000 and 1:10,000 respectively; Millipore). The membranes were then incubated in Immobilon Western HRP Substrate (Millipore) for 5 min and imaged using the Molecular Imager ChemiDoc XRS system (Bio-Rad). Signals were subsequently quantified by densitometric analyses using Quantity One Analysis software (Bio-Rad). The densities of each band, which represented individual animals, were normalized to GAPDH and these normalized values were averaged for control and ic-STZ groups. The data is presented as mean ± SEM. Significance was determine using a two-tailed Student's t-test.

Quantification of GSK-3β phosphorylation

The hippocampus was dissected out and homogenized in chilled Cell Lysis Buffer (Cell Signaling), and clarified by centrifugation at 13,000 x g at 4°C for 10 minutes. The clarified tissue extracts were then stored at -80°C. A BCA protein assay (Pierce, Rockford, IL) was performed to determine protein concentration. Total-GSK-3β and p-GSK-3β solid phase sandwich ELISA kits (Invitrogen) were used and assays were performed according to the manufacturer's protocol. Briefly, standards and samples (1:10 dilution) were run in duplicate on a pre-coated 96-well plate. The absorbance was run on a Synergy HT Spectrophotometer (Bio-Tek) at 450 nm, and KC4 analysis
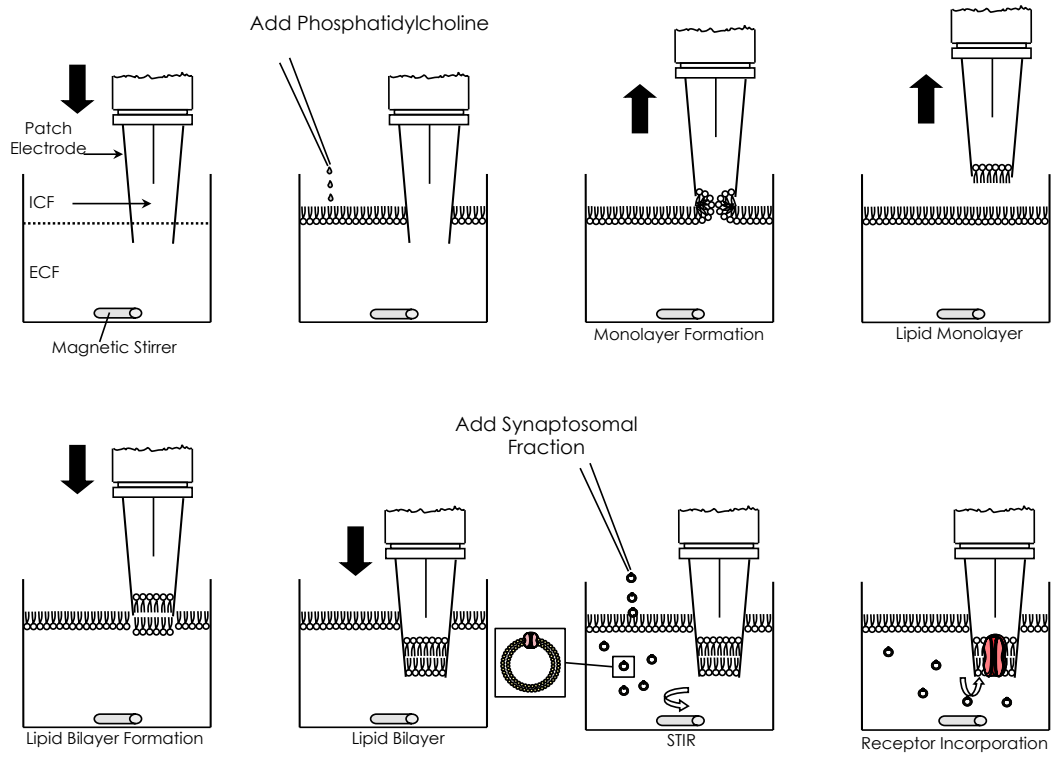
software (Bio-Tek) was used for standard curve fitting (four parameter) and interpolation of absorbance. Duplicates were averaged and the calculated concentrations were normalized to the total protein concentration determined in the BCA assay. p-GSK-3β and Total-GSK-3β values are expressed as mean ± SEM relative to controls, and relative mean p-GSK-3β: relative mean Total-GSK-3β. The data is presented as mean ± SEM. Significance was determine using a two-tailed Student's t-test.

Immunohistochemistry

We performed high-resolution confocal microscopy, focusing on the sratum Radiatum of the CA1. Slices were fixed overnight in 4% paraformaldehyde in phosphate buffer saline, cut in 30μm-thick subslices and transferred to PBS. Sections were washed three times for 10 min in PBS containing 0.1% horse serum. Slices were treated for 1 hour with blocking solution containing 2% horse serum and 0.2% Triton X100 in PBS, followed by 3 hour incubation with monoclonal rabbit antibody against ILK at room temperature. Sections were then washed three times for 10 min in PBS containing 0.1% horse serum. A secondary anti-rabbit IgG antibody coupled to Alexa-Fluor-488 (Invitrogen) (1:200) was applied for 1 hour at room temperature. Finally, sections were rinsed three times for 10 min in PBS containing 0.1% horse serum and mounted in Anti-fade (Invitrogen). Images of stained sections were acquired by a Zeiss 40x objective of a confocal laser scanning microscope. Images were collected sequentially (z-stack). The excitation lasers was 488 nm.

Figure 3-1. Tip-dip patch clamp technique for recording single channel currents from synaptosomal AMPA receptors.

Figure 3-1.

Add Phosphatidylcholine

Patch
Electrode

ICF

ECF

Magnetic Stirrer

Monolayer Formation

Lipid Monolayer

Lipid Bilayer Formation

Lipid Bilayer

Add Synaptosomal
Fraction

STIR

Receptor Incorporation

Table 1-1: Primer sequences for RT-PCR

Gene	Sense (5'-3')	Antisense (5'-3')
β-actin	GGTCGTACCACTGGCATTGTG	GCTCGGTCAGGATCTTCATGAG
ILK1	TCGATGAAGATATGACTGCCC	CAGTGCCACCTTCATCCC
NR1	CTGCAACCCTCACTTTTGAG	TGCAAAAGCCAGCTGCATCT
NR2A	GACGGTCTTGGGATCTTAAC	GACCATGAATTGGTGCAGG
NR2B	CAAGAACATGGCCAACCTGT	GGTACACATTGCTGTCCTTC
GluR1	TTCCTGTTGACACATCCAATCAAT	ATGGTCGATAATGCTAATGAGAGCTT
GluR2	CCTAGCTTCCCAACAGATGGC	GAGGTATGCGAACTTGTCCCA

CHAPTER IV:

RESULTS

Basal Synaptic Transmission and LTP

Input-output relations were constructed to assess the strength of synaptic transmission in the insulin resistant brain of ic-STZ rats. These animals had a significant reduction in fEPSP slope across a range of stimulus intensities (Fig. 4-1A; $p<0.01$; n=9). However, the presynaptic fiber volley amplitude was not significantly different from control slices (Fig. 4-1B; $p>0.05$; n=9), indicating no impairment in conversion of the presynaptic stimulus into axonal depolarization. In figure 4-1C, the fEPSP slope corresponding to a given fiber volley amplitude is shown. The fiber volley indirectly represents the number of axons activated; therefore, this analysis demonstrates that for the same amount of presynaptic input, ic-STZ rats exhibit significantly decreased postsynaptic responses ($p<0.05$; n=9). These depressed responses could be due to decreased probability of release (P_r). To test whether brain-insulin resistance affects P_r, we analyzed the level of paired pulse facilitation (PPF) across a range of inter-stimulus intervals. PPF, a transient form of presynaptic short-term plasticity, and occurs subsequent to an increased probability of synaptic vesicle release. PPF occurs as an enhancement in a fEPSP in responses to a second stimulus timed in close proximity to the first stimulus. The mechanism underlying this effect is believed to involve residual

calcium from the first stimulus which then is augmented by a second stimulus, thereby causing increased vesicle release and a facilitated fEPSP as a final outcome (Wu and Saggau, 1994). In both groups, the fEPSP slope was significantly higher in the second response ($p<0.05$). Moreover, the slope2/slope1 PPF ratio was not significantly different across varied inter-pulse intervals (Fig. 4-1E; $p>0.05$; n=9), indicating that P_r is not altered in ic-STZ animals.

To examine synaptic plasticity in hippocampal slices from control and ic-STZ rats, we induced long-term potentiation (LTP) with high frequency stimulation (3, 100 Hz trains of 100 pulses, with an inter-train interval of 20 seconds). We found that LTP was significantly impaired in the CA1 of ic-STZ rats (Fig. 4-2; $p<0.001$, n=9). In 9 of 9 control rats, LTP could be induced and had an average of 148.67±3.44% normalized to baseline fEPSP slope fifty minutes following HFS; however, in 7 of 9 ic-STZ rats, LTP could not be induced, and averaged 105.99±1.80% fifty minutes after HFS.

The effects of brain-insulin resistance on within-train facilitation were evaluated by measuring the fEPSP amplitudes of responses 2-4 and 98-100, and these values were then normalized to the amplitude of the first response of each respective train. The normalized magnitudes of responses 2-4 and 98-100 were significantly reduced in ic-STZ brains compared to control (Fig. 4-3C,D,E; $p<0.05$ and $p<0.01$ respectively; n=9). To assess tetanic train facilitation in slices from ic-STZ animals, we measured the composite area of each HFS train, and normalized these values to the first train. Control slices demonstrated a significant facilitation of each successive train with respect to the

previous (Fig. 4-3B; *p*<0.05; n=9); however, this effect was absent in ic-STZ tetanic trains. Representative traces are shown in figure 4-3A.

AMPA receptor function

Whole cell patch-clamp recordings were performed in pyramidal neurons of the CA1 region of the hippocampus. Representative traces from control and ic-STZ groups are shown in figure 4-4A. We recorded spontaneous AMPAR-mediated miniature EPSCs in the presence of tetrodotoxin (1μM), a sodium channel blocker. NMDAR activity was inhibited by APV (50μM), and GABAergic inhibition was blocked by picrotoxin (50μM). The amplitude of AMPAR mEPSCs was significantly decreased from 17.82±1.13 pA in controls to 5.48±1.5 pA in icSTZ rats, consistent with the leftward shift of the cumulative distribution of amplitudes in the ic-STZ group (Fig. 4-4B; *p*<0.05; n=6). The change in AMPAR mediated current can be explained by either decreased conductance of the individual AMPA receptors, decreased probability of opening (Po) or a change in surface expression of AMPA receptors at the postsynaptic density. The frequency of AMPAR mediated quantal events was not altered (Fig. 4-4C; 0.38±0.13 Hz in controls and 0.36±0.09 Hz in icSTZ). Since a mEPSC event reflects the release of a single synaptic vesicle, a decreased frequency of events most often correlates to decreased probability of release from the presynaptic terminal. Therefore, this data suggests that presynaptic release is not altered in ic-STZ animals.

We compared the rise time and decay time of AMPAR-mediated mEPSCs. icSTZ rats displayed significantly shorter decay times (Fig. 4-4E; 10.86±0.61 ms in controls and

6.98±0.29 in icSTZ; $p<0.05$; n=6). The time course of quantal synaptic currents depends on a number of factors, at glutamatergic synapses, where neurotransmitter clearance is rapid, the decay time is determined primarily by kinetic properties of the individual receptors (Magleby and Stevens, 1972; Katz and Miledi, 1973). A reduction in the decay time in glutamatergic neurons may reflect desensitization of the receptor or changes in kinetics of channel closure (possibly mediated by splicing variants), and this suggests a depression of synaptic transmission through postsynaptic AMPARs. We found no change in rise time in icSTZ rats (Fig. 4-4D; 2.53±0.09 ms in controls and 2.37±0.06 ms in icSTZ). Mean values for amplitude, frequency, rise time and decay time are summarized in table 4-1.

Single Channel Recordings from Synaptosomal AMPA Receptors

Synaptosomes were isolated from hippocampi of ic-STZ and sham infused rats four weeks following infusion (sixteen weeks of age). The ic-STZ synaptosomes demonstrated significant alterations in the probability of opening (P_o) (Fig. 4-5), as well as open and closed dwell times (Fig. 4-5 and table 4-2). Single channel synaptic AMPA receptor activity was elicited by 290 nM of AMPA in the presence of blockers for Na^+ and K^+ channels, NMDA receptors, kainate receptors, and $GABA_A$ and glycine receptors in extracellular solution (Vaithianathan et al., 2004). These currents were blocked by the antagonist of the AMPA/kainate glutamate receptors, CNQX (1 μM). All-points current amplitude histograms for the steady state probability of observing two current levels were fitted using Gaussian functions (Fig. 4-5). At 290 nM of AMPA, two conductance levels were observed in control and ic-STZ synaptosomes. The principle conductance level of

controls was the higher, 27 pS conductance, while the principle level of the ic-STZ animals was the 14 pS conductance level (Fig. 4-5). This indicates a shift from higher conductance states which is a unique property of AMPA receptors that is known to be regulated by CaMKII alone.

The open and closed dwell time histograms were analyzed and best fitted with two exponentials for the principle conductance of control synaptosomes (27 pS). This is consistent with what we have previously found and reported in synaptosomes from similarly aged animals (Vaithianathan et al., 2004). As shown in table 4-2, synaptosomal AMPA receptors from ic-STZ hippocampi had a significant alteration in the long closed time and a significant reduction in the long open time compared to control synaptosomes (Fig 4-5).

AMPA and NMDA Receptor Expression

Changes in AMPAR subunit composition would have a profound effect on the probability of opening and single channel kinetics; therefore, using western immunodetection we tested this possibility by quantifying the protein levels of GluR1 and GluR2 in whole hippocampal homogenates. However, these experiments revealed no significant changes in the protein levels of GluR1 and GluR2, although a significant reduction in stargazin, the AMPAR auxiliary protein stargazin, was observed (Fig. 4-7D; $p<0.001$). To test whether these results correlated to the expression levels in the synaptic compartment, we repeated the experiments on the synaptoneurosomal fraction and found that GluR1 protein levels were significantly decreased (Fig. 4-7D; $p<0.001$). To verify that mRNA levels in whole hippocampal lysates reflected the protein expression, we also

used RT-PCR to quantify mRNA levels in whole hippocampal lysates. These experiments revealed that GluR1 and GluR2 mRNA levels were unchanged in whole hippocampal lysates (Fig. 4-7E).

Although the aim of this study was focused on AMPAR physiology in these animals, the results from the previous set of experiments prompted us to examine and compare the subunit expression of the NMDAR subunits NR1, NR2A, and NR2B in whole hippocampal homogenates versus the synaptoneurosome fraction of the hippocampus. There were significantly increased levels of NR1 mRNA (Fig. 4-7C; $p<0.05$); however, protein levels in the synaptoneurosome fraction were decreased (Fig. 4-7A; $p=0.0586$). There was a significant reduction of NR2B mRNA levels (Fig. 4-7C; $p<0.0001$), which correlated with a significant decrease of NR2B protein (Fig. 4-7A; $p<0.001$). Interestingly, there was a slight but non-significant reduction in NR2A mRNA ($p>0.05$; Fig. 4-7C), and a large reduction of NR2A protein content ($p<0.0001$; Fig. 4-7A).

Signaling and Expression of the ILK-GSK-3β Pathway

The activity of GSK-3β, which is dependent on the phosphorylation state of the enzyme, has a dramatic influence on synaptic plasticity; therefore, we performed a solid phase sandwich ELISA to quantify the level of GSK-3β phosphorylated at the serine-9 residue (p-GSK-3β). A separate ELISA was also performed to detect the level of total GSK-3β, which was used to normalize the level of p-GSK-3β. The results are expressed as the normalized (to control) ratio of p-GSK-3β:Total-GSK-3β. The ratio of p-GSK-3β:Total-GSK-3β was significantly ($p<0.0001$; n=8) reduced to 65.18±4.08% in ic-STZ

animals compared to control (100±1.59%), indicating increased levels of active GSK-3β in ic-STZ synaptoneurosomes (Fig. 4-8C). The two major kinases involved in the regulation of GSK-3β are Integrin-linked kinase (ILK) and Akt. Therefore, we set out to determine the levels of phosphorylated Akt (p-Akt) and the protein and mRNA levels of ILK. There was no change in the ratio of p-Akt:Total-Akt in the synaptoneurosomal fraction of the hippocampus. Conversely, ILK mRNA levels were significantly reduced in the hippocampus of ic-STZ rats (Fig. 4-8B; p,0.01; n=6), which correlated to significantly decreased protein levels in the synaptoneurosome fraction (Fig. 4-8A; $p<0.05$; n=6). BDNF is an essential mediator of LTP (Kang et al., 1997) and is also known to modulate GSK-3β activity (Mai et al., 2002; Bachmann et al., 2005). There was no change in pro-BDNF protein levels in ic-STZ animals; however, there was a substantial loss of mature-BDNF (Fig. 4-8D; $p<0.0001$; n=6).

Immunohistochemical staining of ILK in the CA1 of the hippocampus from control and ic-STZ animals revealed uniform distribution of ILK and intense staining throughout the dendritic shaft and spine head (arrow) in controls, and abnormal clustered distribution and lack of dendritic staining of ILK in the ic-STZ hippocampus. Furthermore, the overall intensity of ILK immunoreactivity is decreased in images from ic-SZ animals relative to control (Fig. 4-10). This supports our expression analysis of ILK and suggests that the localization of ILK may be altered in ic-STZ animals.

Acute PPAR-δ agonist treatment partially rescues synaptic deficits

The PPAR-δ agonist GW501516 (10 mg/kg) or the PEG vehicle was administered to ic-STZ animals three hours prior to sacrifice, and following sacrifice hippocampal

slices were produced for extracellular field recordings. The average fEPSP slope for the vehicle treated ic-STZ group was significantly reduced at all stimulus levels compared to vehicle treated control (Fig. 4-8A; $p<0.01$; n=4), and this was partially rescued in the GW501516 treatment group; slope values for this group were significantly different than both the control and ic-STZ groups (Fig. 4-8A; $p<0.05$; n=4). There was no significant difference between the fiber volley at any stimulus intensity (Fig. 4-8B). However, the fEPSP slope plotted as a function of fiber volley was significantly reduced in vehicle treated ic-STZ animals (Fig. 4-8C; $p<0.05$; n=4), the GW501516 treatment group was not significantly different than vehicle treated controls (Fig. 4-8C; $p>0.05$; n=4).

LTP was induced by high frequency stimulation (3 trains of 100 pulses (100 Hz), with 20 sec. intertrain interval) in vehicle treated control animals, and consistent with our previous data, failed to do so in the vehicle treated ic-STZ group. Acute administration of GW501516, the selective PPAR-δ agonist, partially rescued LTP three hours following IP injection. Normalized fEPSP slopes 50 min post-HFS averaged 148.67 ±3.44% for vehicle treated control, 105.99 ±1.80% for vehicle treated ic-STZ animals and 136.31±1.93% for the GW501516 treated group (Fig. 4-9).

Figure 4-1. Basal synaptic transmission is impaired in ic-STZ animals. **A.** Representative responses from control and ic-STZ animals show a large reduction in fEPSP the ic-STZ group (Scale bars = 0.3 mV/5 ms). B**.** The average fEPSP slope for ic-STZ (open circles) was significantly reduced at all stimulus levels compared to control (filled circles; $p < 0.01$; n=9). **C.** Average fiber volley amplitude plotted for each stimulus intensity, there was no statistical difference between control and ic-STZ ($p > 0.05$; n=9). **D.** Average fEPSP slopes plotted as a function of the average fiber volley amplitude, for a given fiber volley amplitude, the fEPSP slope obtained was significantly reduced in ic-STZ animals ($p < 0.05$; n=9). **E.** PPF Comparison of paired-pulse facilitation (PPF) in controls (filled squares) and ic-STZ (open circles). PPF ratio (slope2/slope1) in ic-STZ animals measured at different interpulse intervals was not significantly different from controls ($P > 0.05$; n=9).
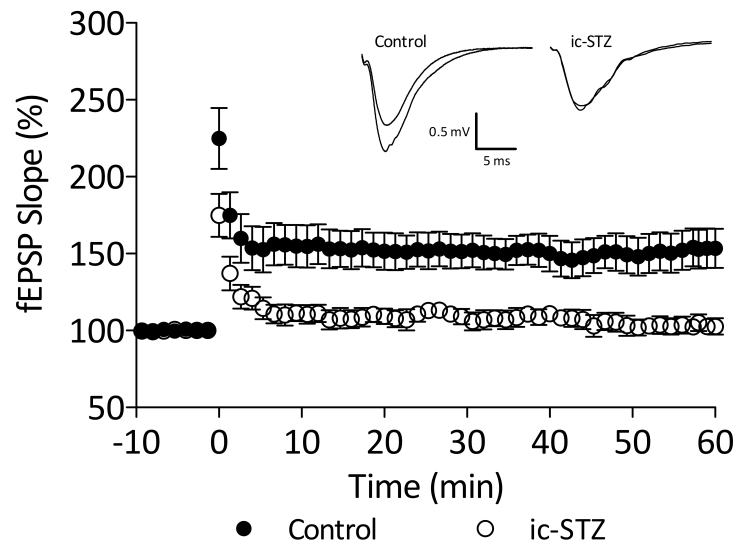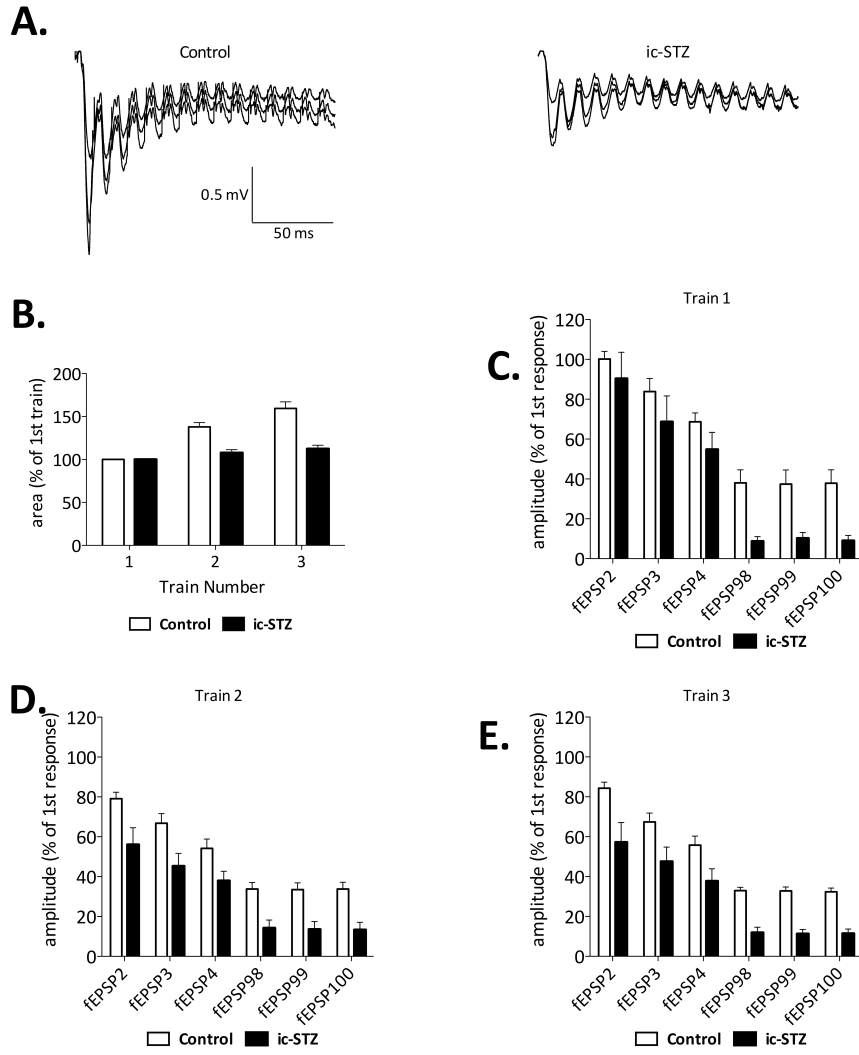
Figure 4-1.
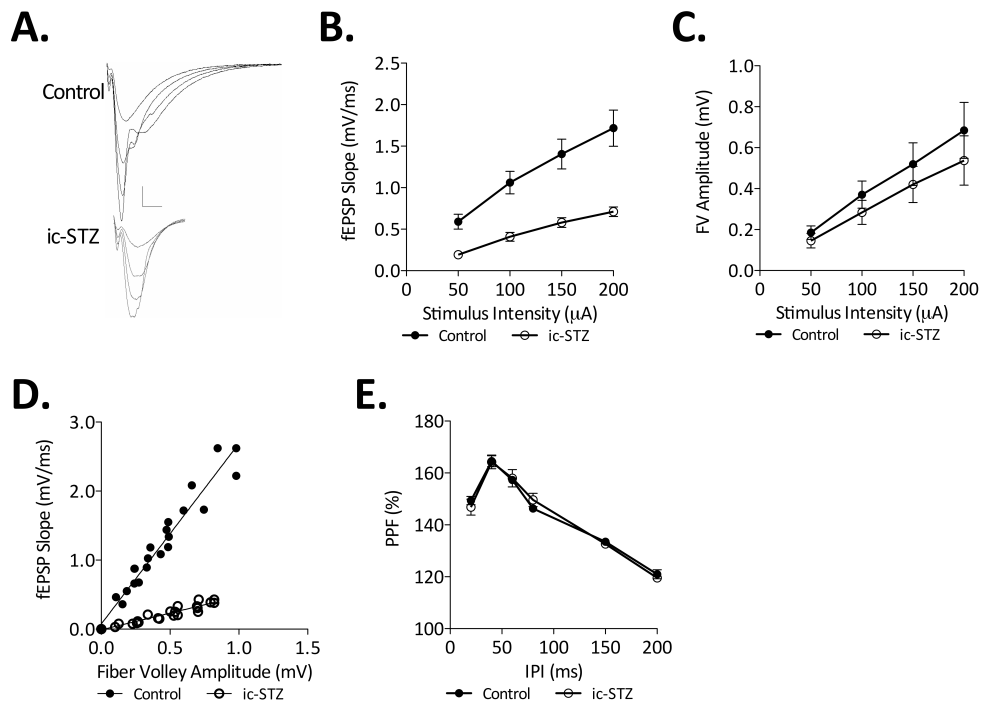
Figure 4-2. LTP was induced by high frequency stimulation (3 trains of 100 pulses (100 Hz), with 20 sec. intertrain interval) in control animals, but failed to do so in the ic-STZ group. Representative traces before and 40 minutes post-HFS are shown for control and ic-STZ animals. Normalized fEPSP slopes 50 min post-HFS averaged 148.67 ±3.44% for control and 105.99 ±1.80% for ic-STZ animals.
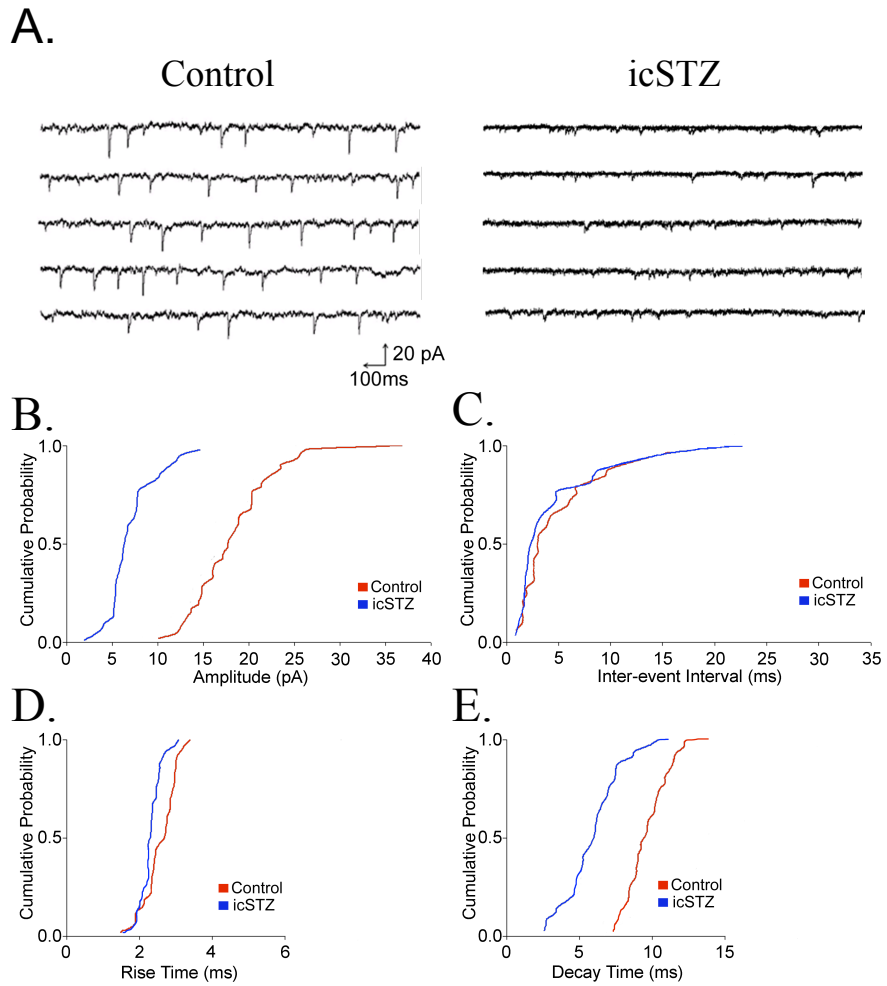
Figure 4-2.

Figure 4-3. Effects of brain insulin-resistance on tetanic stimulation responses. **A.** Representative traces from all three train responses. **B.** Comparison of the composite area of fEPSP responses during each HFS train. The values are expressed as a relative percentage of the first train. In the control but not ic-STZ slices, tetanic facilitation occurred, with each successive train having a significantly larger area than the previous in the control slices ($p<0.05$; n=9). **C,D,E.** The fEPSP amplitudes of the fEPSP amplitudes of responses 2-4 and 98-100 were normalized to the amplitude of the first response of each respective train. The measures are shown for responses 2-4 and 98-100 of each train, noted as Train 1 (**C**), Train 2 (**D**), and Train 3 (**E**) above each figure. Within-train facilitation was significantly decreased in ic-STZ slices ($p<0.01$; n=9).

Figure 4-3.

Figure 4-4. Effect of central insulin resistance on AMPA receptor physiology. AMPA receptor-mediated mEPSCs were recorded in the whole cell mode in the presence of TTX, APV, and bicuculline with the membrane clamped at -70 mV. **A.** Representative traces of mEPSCs from CA1 pyramidal neurons from control and icSTZ hippocampal slices. Cumulative probability distributions of **B.** amplitude, **C.** interevent intervals, **D.** rise time, and **E.** decay time are show. Distributions for amplitude and decay time are shifted to the left in icSTZ animals corresponding to the change in amplitude from 17.82±1.13 pA in controls to 5.48±1.5 pA in icSTZ rats, and the change in decay time from 10.86±0.61 ms to 6.98±0.29. mEPSC frequency (0.38±0.13 Hz in controls and 0.36±0.09 Hz in icSTZ) and rise time (2.53±0.09 ms in controls and 2.37±0.06 ms in icSTZ) were not significantly different between control and icSTZ groups.
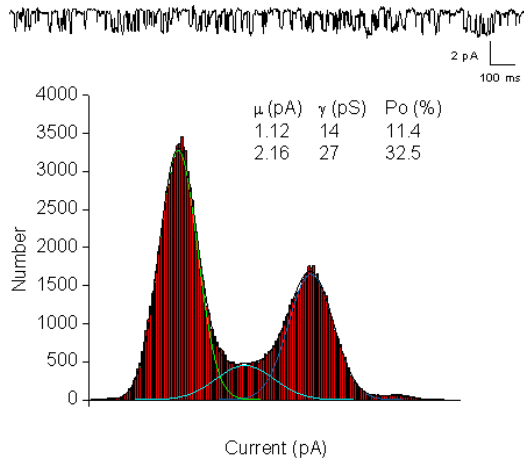
Figure 4-4.

Figure 4-5. Single channel properties of synaptosomal AMPA receptors. Representative traces occurring at -80 mV in the presence of 290 nM AMPA, 50 μM AP5, 1 μM TTX, 2 μM TEA and 100 μM picrotoxin are shown for **(A)** control and **(B)** icSTZ synaptosomes. The channel conductance levels and relative occurrence of open states of AMPA receptor currents are 14 pS, (11.4%), 27 pS (32.5%) for controls and 14 pS, (5.4%), 27 pS for ic-STZ synaptosomes. The single channel open and close time distributions are shown for **(A)** control and **(B)** ic-STZ synaptosomes. These histograms of duration of openings and closures were fitted with two exponentials by Marquardt least squares methods. The summary of these fittings is shown in table 4-3.
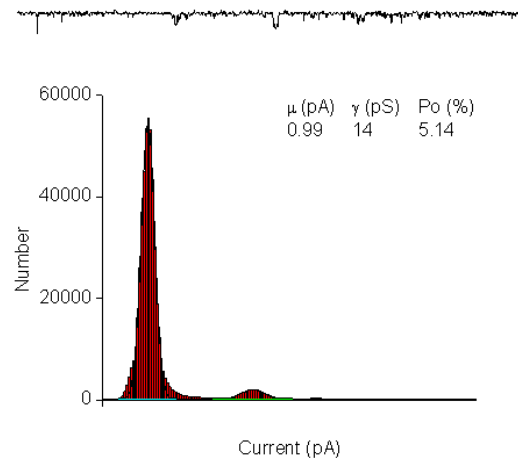
Figure 4-5.
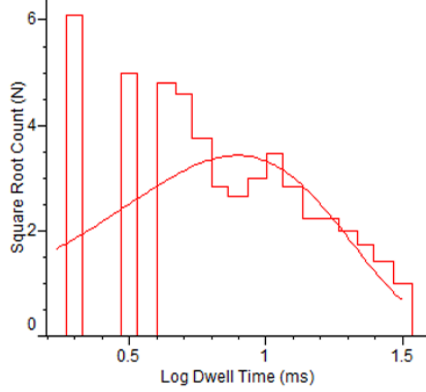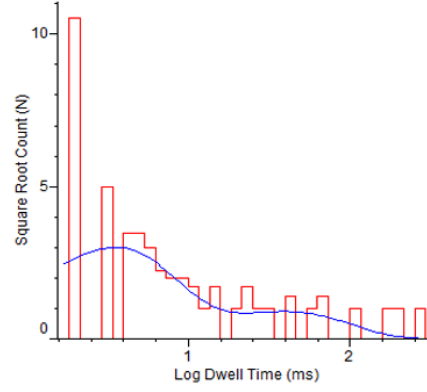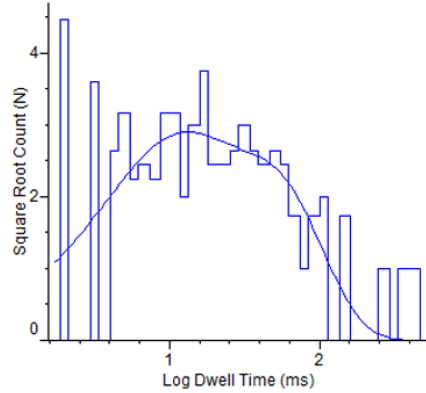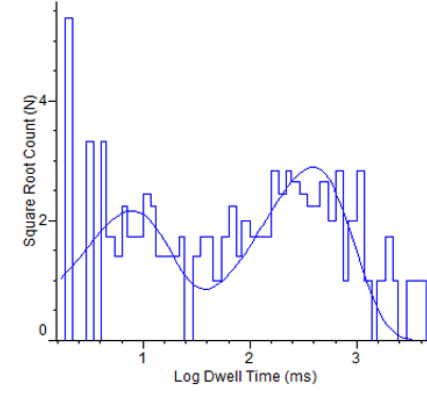
Figure 4-6. Western Blot analysis of protein levels of **A.** NR1, NR2A, and NR2B NMDAR subunits and **D.** GluR1 and GluR2 AMPAR subunits and the AMPAR-interacting protein stargazin was performed in the synaptoneurosome fraction of the hippocampus from control (Con) and ic-STZ (icSTZ) rats. **B.** The density of NR2A and NR2B protein levels were normalized to GAPDH and are expressed as a ratio of NR2A:NR2B in control and ic-STZ rats. mRNA levels of **C.** NR1, NR2A, and NR2B and **E.** GluR1 and GluR2 levels were quantified using rt-PCR. The quantitative data of protein and mRNA levels are expressed as a percentage of the control group, which was set as 100%. Bar graphs show mean±SEM from 8 animals per group. *** $p < 0.001$, ** $p < 0.001$, and * $p < 0.05$ (two-tailed, unpaired Student's t-test). Representative samples are shown.

Figure 4-6.
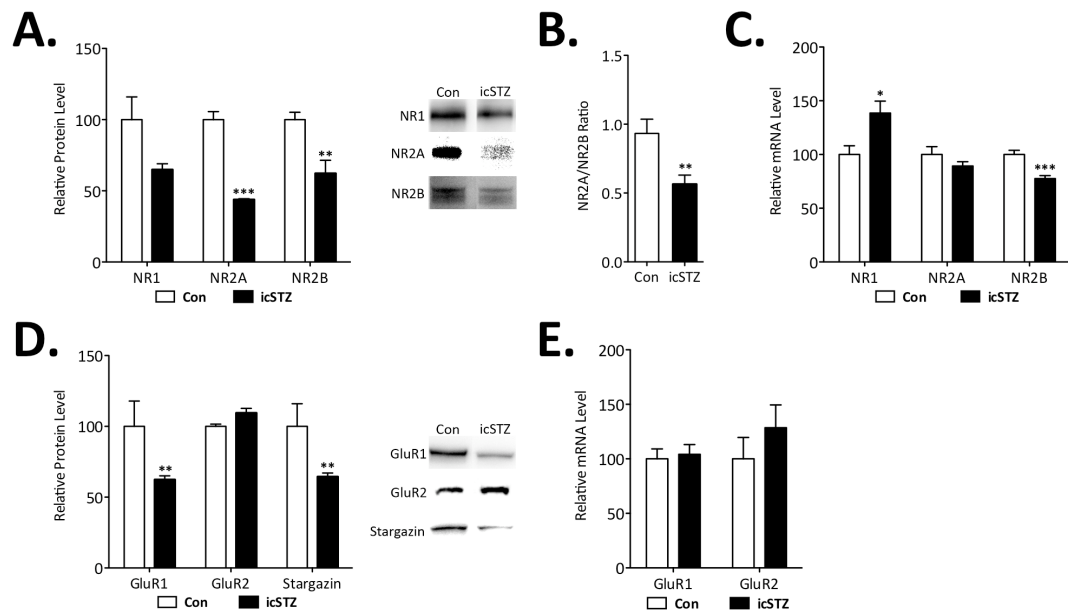
Figure 4-7. Examination of GSK3-β signaling and BDNF expression in the synaptoneurosomal fraction of control and ic-STZ hippocampus. **A,C.** Protein levels of ILK, proBDNF, and mature-BDNF (mBDNF) were quantified by western blot analysis and were normalized to GAPDH. **B.** Densitometric values for total-Akt obtained by western blot were normalized to GAPDH and phospho-Akt (Ser473) was normalized to total (**C.**) Phospho-GSK3-**β** (Ser9) and total-GSK3β levels were quantified by sandwich ELISA and phospho-GSK3-β was normalized to total. The quantitative data of protein levels are expressed as a percentage of the control group, which was set as 100%. Bar graphs show mean±SEM from 8 animals per group. *** $p<0.001$, ** $p<0.001$, and * $p<0.05$ (two-tailed, unpaired Student's t-test). Representative samples are shown.

Figure 4-7.
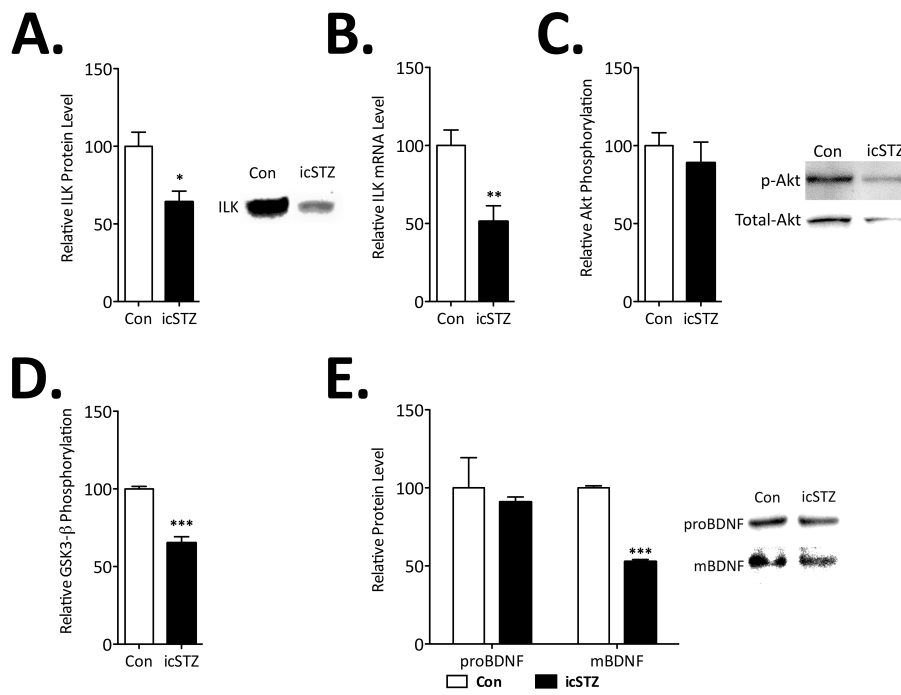
**Figure 4-8.** Impaired basal synaptic transmission in ic-STZ rats is partially rescued by PPAR-δ activation. Rats were treated with a single IP injection of either GW501516 (10 mg/kg; ic-STZ+GW501516) or an equal volume of vehicle (control, ic-STZ). The animals were sacrificed three hours post treatment **A.** The average fEPSP slope for the vehicle treated ic-STZ group (open circles) was significantly reduced at all stimulus levels compared to vehicle treated control (filled circles; $p<0.01$; n=4), and this was partially rescued in the GW501516 treatment group; slope values for this group were significantly different than both the control and ic-STZ groups (open squares; $p<0.05$; n=4). **B.** Average fiber volley amplitude plotted for each stimulus intensity, there was no statistical difference between any group ($p>0.05$; n=4). **C.** Average fEPSP slopes plotted as a function of the average fiber volley amplitude, for a given fiber volley amplitude, the fEPSP slope obtained was significantly reduced in vehicle treated ic-STZ animals (red linear regression line; $p<0.05$; n=4), the GW501516 treatment group (blue linear regression line) was not significantly different than vehicle treated controls (black linear regression line; $p>0.05$; n=4). **D.** PPF Comparison of paired-pulse facilitation (PPF) in vehicle treated controls (filled squares), vehicle treated ic-STZ (open circles) and ic-STZ rats treated with GW501516 (open squares). PPF ratio (slope2/slope1) measured at different interpulse intervals was not significantly between groups (P>0.05; n=4).

Figure 4-8.

A.

B.

C.

D.
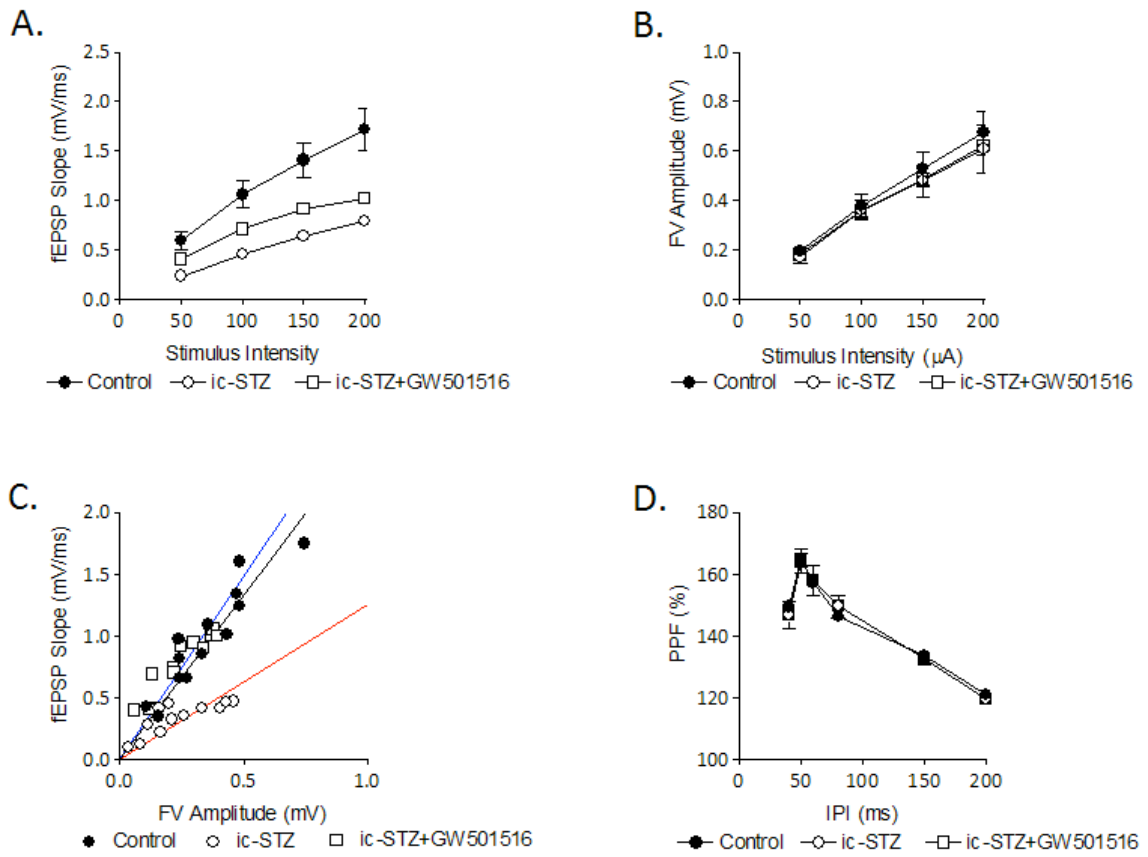
Figure 4-9. LTP was induced by high frequency stimulation (3 trains of 100 pulses (100 Hz), with 20 sec. intertrain interval) in vehicle treated control animals, and consistent with our previous data, failed to do so in the vehicle treated ic-STZ group. Acute administration of GW501516, the selective PPAR-δ agonist, partially rescued LTP three hours following IP injection. Normalized fEPSP slopes 50 min post-HFS averaged 148.67 ±3.44% for vehicle treated control, 105.99 ±1.80% for vehicle treated ic-STZ animals and 136.31±1.93% for the GW501516 treated group.

Figure 4-9.
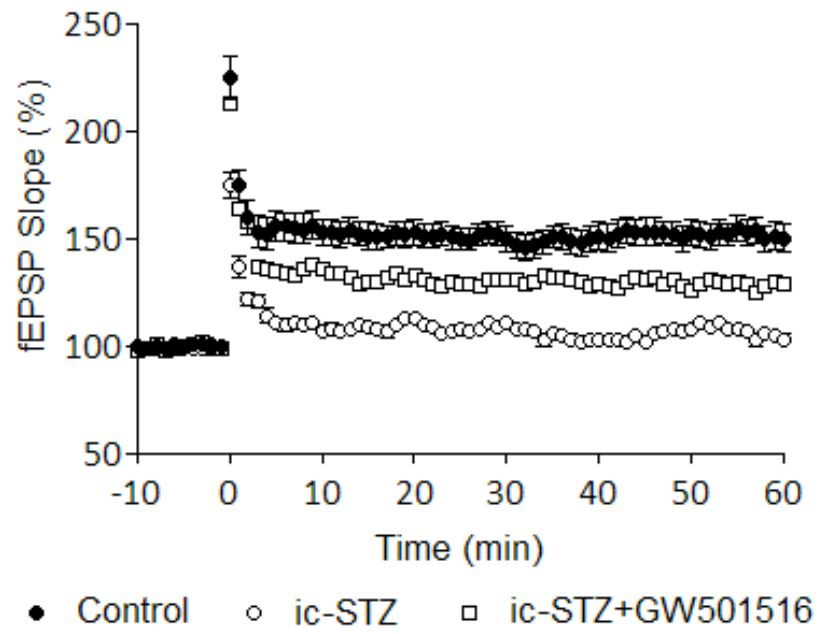
Figure 4-10. Immunohistochemical stain of ILK in the CA1 of the hippocampus from control and ic-STZ animals. Control sections show uniform distribution of ILK and intense staining throughout the dendritic shaft and spine head (arrow) in controls, and abnormal clustered distribution and lack of dendritic staining of ILK in the ic-STZ hippocampus. Furthermore, the overall intensity of ILK immunoreactivity is decreased in images from ic-SZ animals relative to control.

Figure 4-10.
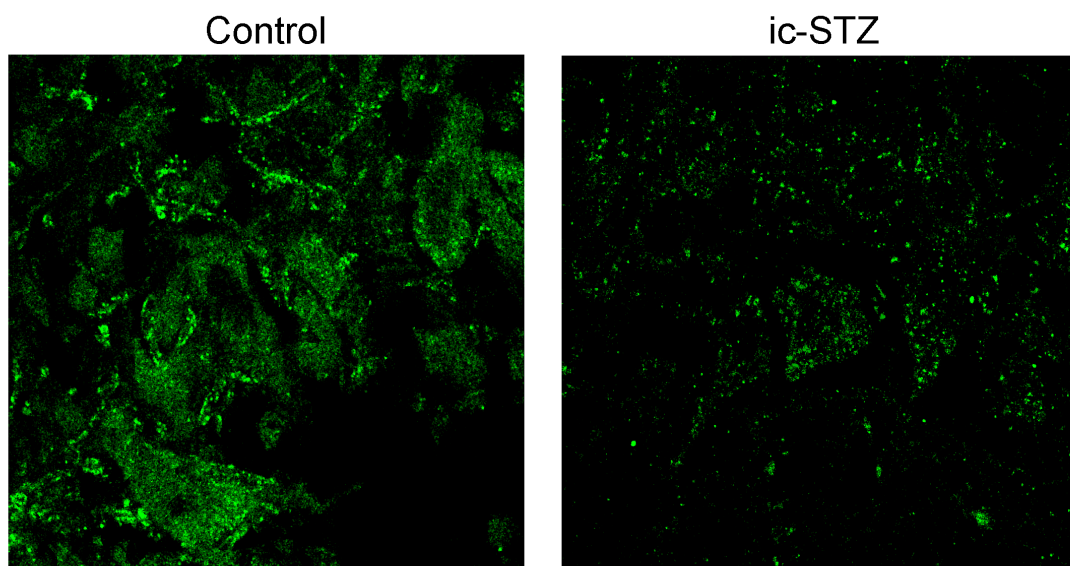
Control   ic-STZ

Table 4-1: AMPAR-mediated mEPSC Properties

	Control	ic-SZ	% Change
Amplitude (pA)	17.82 ± 1.13	5.48 ± 1.5*	-69.25
Frequency (Hz)	0.38 ± 0.13	0.36 ± 0.09	-
Rise Time (ms)	2.53 ± 0.09	2.37 ± 0.06	-
Decay Time (ms)	10.86 ± 0.61	6.98 ± 0.29*	-35.73

Results are expressed as mean ± SD. * p <0.05 relative to control experiments.

Table 4-2: AMPAR Single Channel Open-Closed Time Properties

	Control	ic-STZ
Close Time (ms)	40.24 ± 0.30 (59.9 ± 0.016%)	78.73 ± 0.14* (59.0 ± 0.06%)
	7.37 ± 0.47 (40.1 ± 0.15%)	7.28 ± 0.21 (41.0 ± 0.06%)
Open Time (ms)	0.53 ± 0.63 (2.3 ± 0.32%)	0.48 ± 0.57 (13.6 ± 0.33%)
	7.87 ± 0.25 (97.7 ± 0.17%)	3.8 ± 0.37* (86.4 ± 0.21%)

Results are expressed as mean ± SD. * p <0.05 relative to control experiments.

CHAPTER V:

DISCUSSION

Once we established that these animals did in fact have deficits in plasticity, we then attempted to begin to describe a mechanism accounting for these observations. To this end, we performed whole cell patch clamp recordings of isolated AMPA receptor synaptic currents in CA1 pyramidal neurons of the hippocampus. The results of these experiments revealed a profound deficit in AMPA receptor-mediated currents. The change in AMPAR mediated current can be explained by a change in the functional properties of the individual AMPA receptors or a change in surface expression of AMPA receptors on the postsynaptic membrane. To determine whether the decreased AMPA receptor amplitudes were due to changes in the single channel properties, we performed single channel recordings from synaptosomal AMPA receptors isolated from the hippocampus of icSTZ rats. We found significant changes in receptor opening and receptor kinetics, and based on the analysis of these recordings hypothesized that an alteration in AMPA receptor subunit composition may underlie these changes. Therefore, using western immunodetection we tested this possibility by quantifying the protein levels of GluR1 and GluR2 in the hippocampus. We compared subunit expression in the synaptosomal fraction versus whole cell lysates and found that while

GluR1 and GluR2 protein levels in the entire cytosolic fraction were not altered, there was a significant reduction in GluR1 content in the synaptic compartment. This suggests that GluR1 trafficking is perturbed in the neurons of these animals. The composition of AMPARs has a dramatic effect on synaptic plasticity. Whereas GluR2 containing receptors have low calcium permeability and have outwardly rectifying properties, GluR1 containing AMPARs have high calcium permeability and have an inwardly rectifying IV relationship (Hollmann et al., 1991; Burnashev et al., 1992). This hypothesis was supported by experiments using RT-PCR to quantify the mRNA content of GluR1 and GluR2, which were not significantly different from controls. We speculate that the discrepancies between mRNA and protein levels may involved disrupted cellular trafficking to the synapse, and may involve improper protein translation and post-translational events. Although not fully understood, it is believed that mRNA transcripts are trafficked to the dendritic compartment where they are locally translated. Based on this we speculate that insulin signaling might play some role in regulating or maintaining basal mRNA trafficking of GluR1 transcripts. Furthermore, the reduction in the transmembrane AMPA receptor regulatory protein stargazin suggests possible changes in AMPARs trafficking as well as single channel properties as this protein is known to play essential roles in both (Priel et al., 2005) (Bats et al., 2007).

The changes in glutamate receptor expression that occur in ic-STZ animals are in contrast to the previously reported up-regulation of these proteins in spontaneous type-I diabetic animals (Valastro et al., 2002), and the lack of change during early time points occurring in systemically administered STZ rats (Gardoni et al., 2002). This interesting

difference suggests that although insulin deficiency and insulin resistance both result in memory impairment, it is likely that the two are mediated by different underlying mechanisms. Epidemiologic evidence that type-2 diabetes is a major risk factor for AD suggests an involvement of insulin signaling in synaptic physiology. Previous studies have reported decreased IR expression and IR desensitization in AD brains (Hoyer, 2004; Steen et al., 2005); furthermore, since AD is also associated with decreased glutamate receptor levels (Bi and Sze, 2002), our results add to the emerging evidence that brain-insulin resistance may be a key feature of AD pathology.

Our next aim was to begin to connect insulin signaling to synaptic plasticity. The insulin signaling pathway and synaptic plasticity signaling mechanisms shares several common molecules, therefore, it seemed logical to start building a working model by investigating the activity and expression of these molecules in the ic-STZ hippocampus. We utilized several biochemical techniques to detect changes in GSK-3β, Akt, integrin-linked kinase (ILK), BNDF and Erk-1/2 at the transcriptional, translational and posttranslational levels. The results of these studies suggest a novel role for ILK in synaptic plasticity and provide preliminary evidence implicating a role for ILK in neurodegeneration, although further investigation is necessary to substantiate this postulate.

Insulin receptors are present on the synaptic membrane and activate Akt and ILK in a PI3K-dependent manner. There is evidence emerging from multiple reports that indicates that insulin-signaling pathways are impaired in the Alzheimer's disease brain (Frolich et al., 1999; Rivera et al., 2005; Cole and Frautschy, 2007; Neumann et al.,

2008). ILK associates with the intracellular domain of β1-integrins. The only upstream molecule that can directly regulate the activity of both Akt and GSK-3β is (ILK) (Naska et al., 2006). Therefore, because of this unique ability of ILK along with the reports that β1-integrin knock out mice have deficits in LTP and AMPA receptor transmission, we hypothesized that changes in ILK may be involved in the impairments we observed in the ic-STZ hippocampus. In the hippocampus, Akt and ILK are the primary kinases involved in the phosphorylation of glycogen synthase kinase or GSK-3beta. This phosphorylation decreases GSK activity, which was recently demonstrated to be necessary for the insertion of GluR1 containing receptors during the induction of LTP.   Therefore, since reduced IR, expression and binding affinity are known to be present in the brains of ic-STZ animals, we investigated the expression and activity of GSK3-β, Akt and ILK. Our results indicate that a significant increase in GSK3-β activity occurs, which is correlated to a deficiency in ILK expression, and there was no significant change in the activity of Akt. There are also reports that ILK plays a role in maintaining BDNF expression in the hippocampus, although the mechanism for this phenomenon is unknown. Nevertheless, this suggests another means by which ILK downregulation may play a role in the LTP deficits we observed in the icSTZ animals.   We found that while proBDNF was unchanged, the level of mature BDNF was decreased in icSTZ animals.

These findings suggest a novel role of ILK in synaptic physiology, and for the first time may implicate a pathologic function of this kinase in neurological disease. Further studies are warranted to validate and characterize the importance of ILK in synaptic plasticity and neurodegenerative disease. ILK plays an important role in the

regulation of actin cytoskeleton dynamics (Blattner and Kretzler, 2005), which is known to play a role in AMPA receptor trafficking and spine morphological changes during synaptic plasticity. Since ILK links integrins to the actin cytoskeleton, and because of the importance of the cytoskeleton in AMPA receptor synaptic transmission (Kim and Lisman, 1999), LTP (Kim and Lisman, 1999; Krucker et al., 2000), and AMPA surface expression (Zhou et al., 2001) we hypothesize that ILK may play an essential role in synaptic plasticity through this mechanism. ILK signaling is also essential for maintaining the expression of brain-derived neurotrophic factor (BDNF) (Guo et al., 2008) and we can speculate that deficits in ILK may be responsible for the decreased BDNF expression reported in the present study. A working model is proposed in figure 5-1.

GSK3-β activation is responsible for increased tau hyperphosphorylation, the primary component of neurofibrillary tangles in AD brains. Previous studies have shown increased hyperphosphorylated tau in ic-STZ brains, which are in line with our results and further support the hypothesis that central insulin resistance may be a primary cause of AD pathology. Findings published in the last year have now directly implicated GSK-3β in the regulation of hippocampal synaptic plasticity. These findings report that GSK3-β activity is inhibited during the induction of LTP in the hippocampus. Based on this, it is not surprising that LTP is impaired in a transgenic mouse with GSK-3β overexpression, which displays enhanced GSK-3 activity. Moreover, these LTP deficits can be attenuated by treatment with various GSK-3β inhibitors such as lithium. It has also recently been revealed that GSK-3β directly complexes with AMPA receptors, the

primary receptor responsible for LTP, and regulates the surface expression of these according to its phosphorylation state (Hooper et al., 2007; Peineau et al., 2007; Zhu et al., 2007).

Our data suggests a possible role for the ILK-GSK3-β pathway in synaptic dysfunction in the insulin resistant brain. However, we cannot exclude the contribution of other pathways, and our data in fact suggests that multiple factors may converge via Akt, ILK, BDNF and GSK3-β to modulate glutamatergic transmission. Based on our results, we can therefore, suggest that these modulatory pathways may require a functional insulin signaling system without which severe deficits in synaptic plasticity would occur.

Figure 5-1. Insulin receptors which are present on the synaptic membrane activate AKT in a PI3Kinase-dependent manner. They also activate integrin linked kinase. ILK associates with the intracellular domain of beta-1 integrin receptors. Because of its relationship with the insulin signaling pathways and since beta 1 integrin knock out mice have deficits in LTP and AMPA receptor transmission, we hypothesized that changes in ILK may be involved in the impairments we observed in the icSTZ hippocampus. We found that ILK protein levels were reduced by about 40% in the synaptosome fraction of icSTZ animals. In the hippocampus Akt and ILK are the primary kinases involved in the phosphorylation of glycogen synthase kinase or GSK-3beta. This phosphorylation decreases GSK activity, which Simon Lovestone's group recently demonstrated is necessary for the insertion of GluR1 containing receptors during the induction of LTP. We used a sandwich ELISA to quantify the levels of phosphorylated and total GSK-3 beta, and we found a decreased ratio of GSK-3beta to total GSK. Since phosphorylated GSK is the inactive form a decreased ratio of phospho-GSK to Total-GSK indicates increased levels of active GSK. Since AKT is the other major kinase responsible for the phosphorylation of GSK-3beta, we measured the levels of phosphorylated AKT, and found no significant change. This suggests that the downregulation of ILK may be important to the mechanism of LTP and memory deficits caused by central insulin resistance. There are also reports that ILK plays a role in maintaining BDNF expression in the hippocampus, although the mechanism for this phenomenon is unkonwn. Nevertheless, this suggests another means by which ILK downregulation may play a role in the LTP deficits we observed in the icSTZ animals. We found that while proBDNF was unchanged, the level of mature BDNF was nearly 50% lower in icSTZ animals. ILK is directly linked to the actin cytoskeleton, which is known to play a role in AMPA receptor trafficking and spine morphological changes during synaptic plasticity. Since ILK links integrins to the actin cytoskeleton, and because of the importance of integrins in synaptic plasticity, we hypothesize that ILK may play an essential role in synaptic plasticity through this mechanism, and we are currently investigating this hypothesis in primary hippocampal cultures using RNA interference to specifically knockdown ILK expression. This follow up study will be the first to demonstrate a role for ILK in synaptic transmission and plasticity, and may have implications for disorders of learning and memory.

Figure 5-1
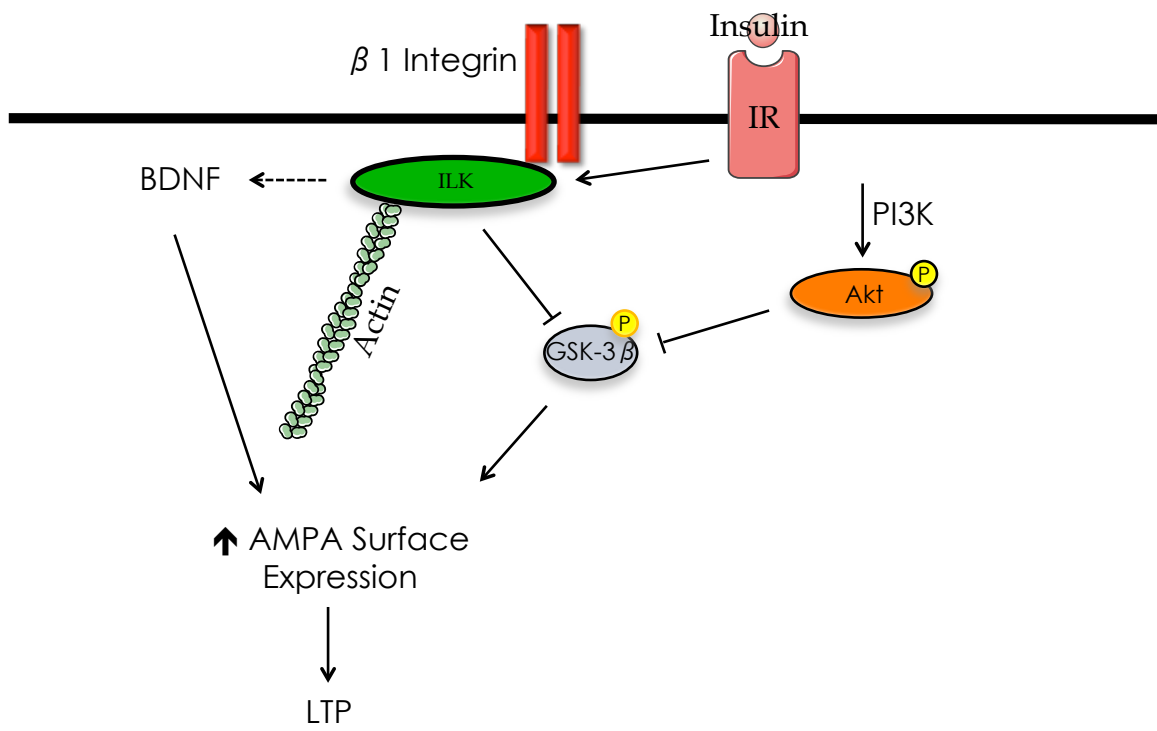
REFERENCES

Abbott MA, Wells DG, Fallon JR (1999) The insulin receptor tyrosine kinase substrate p58/53 and the insulin receptor are components of CNS synapses. J Neurosci 19:7300-7308.

Adams JP, Sweatt JD (2002) Molecular psychology: roles for the ERK MAP kinase cascade in memory. Annu Rev Pharmacol Toxicol 42:135-163.

Adesnik H, Nicoll RA, England PM (2005) Photoinactivation of native AMPA receptors reveals their real-time trafficking. Neuron 48:977-985.

Adlerz L, Holback S, Multhaup G, Iverfeldt K (2007) IGF-1-induced processing of the amyloid precursor protein family is mediated by different signaling pathways. J Biol Chem 282:10203-10209.

Alonso M, Medina JH, Pozzo-Miller L (2004) ERK1/2 activation is necessary for BDNF to increase dendritic spine density in hippocampal CA1 pyramidal neurons. Learn Mem 11:172-178.

Alvarez G, Munoz-Montano JR, Satrustegui J, Avila J, Bogonez E, Diaz-Nido J (2002) Regulation of tau phosphorylation and protection against beta-amyloid-induced neurodegeneration by lithium. Possible implications for Alzheimer's disease. Bipolar Disord 4:153-165.

American Psychiatric Association., American Psychiatric Association. Task Force on DSM-IV. (2000) Diagnostic and statistical manual of mental disorders : DSM-IV-TR, 4th Edition. Washington, DC: American Psychiatric Association.

Anderson WW, Collingridge GL (2007) Capabilities of the WinLTP data acquisition program extending beyond basic LTP experimental functions. J Neurosci Methods 162:346-356.

Anderton BH (1999) Alzheimer's disease: clues from flies and worms. Curr Biol 9:R106-109.

Andreasen N, Blennow K (2002) Beta-amyloid (Abeta) protein in cerebrospinal fluid as a biomarker for Alzheimer's disease. Peptides 23:1205-1214.

Anson LC, Chen PE, Wyllie DJ, Colquhoun D, Schoepfer R (1998) Identification of amino acid residues of the NR2A subunit that control glutamate potency in recombinant NR1/NR2A NMDA receptors. J Neurosci 18:581-589.

Arvanitakis Z, Wilson RS, Bienias JL, Evans DA, Bennett DA (2004) Diabetes mellitus and risk of Alzheimer disease and decline in cognitive function. Arch Neurol 61:661-666.

Atkins CM, Selcher JC, Petraitis JJ, Trzaskos JM, Sweatt JD (1998) The MAPK cascade is required for mammalian associative learning. Nat Neurosci 1:602-609.

Avila J (2004) The influence of aging in one tauopathy: Alzheimer 's disease. Arch Immunol Ther Exp (Warsz) 52:410-413.

Bachmann RF, Schloesser RJ, Gould TD, Manji HK (2005) Mood stabilizers target cellular plasticity and resilience cascades: implications for the development of novel therapeutics. Mol Neurobiol 32:173-202.

Banke TG, Traynelis SF (2003) Activation of NR1/NR2B NMDA receptors. Nat Neurosci 6:144-152.

Barria A, Malinow R (2002) Subunit-specific NMDA receptor trafficking to synapses. Neuron 35:345-353.

Bats C, Groc L, Choquet D (2007) The interaction between Stargazin and PSD-95 regulates AMPA receptor surface trafficking. Neuron 53:719-734.

Beasley C, Cotter D, Khan N, Pollard C, Sheppard P, Varndell I, Lovestone S, Anderton B, Everall I (2001) Glycogen synthase kinase-3beta immunoreactivity is reduced in the prefrontal cortex in schizophrenia. Neurosci Lett 302:117-120.

Beattie EC, Carroll RC, Yu X, Morishita W, Yasuda H, von Zastrow M, Malenka RC (2000) Regulation of AMPA receptor endocytosis by a signaling mechanism shared with LTD. Nat Neurosci 3:1291-1300.

Behe P, Stern P, Wyllie DJ, Nassar M, Schoepfer R, Colquhoun D (1995) Determination of NMDA NR1 subunit copy number in recombinant NMDA receptors. Proc Biol Sci 262:205-213.

Benedict C, Hallschmid M, Schultes B, Born J, Kern W (2007) Intranasal insulin to improve memory function in humans. Neuroendocrinology 86:136-142.

Bhat RV, Budd Haeberlein SL, Avila J (2004) Glycogen synthase kinase 3: a drug target for CNS therapies. J Neurochem 89:1313-1317.

Bhattacharya SK, Saraswati M (1991) Effect of intracerebroventricularly administered insulin on brain monoamines and acetylcholine in euglycaemic and alloxan-induced hyperglycaemic rats. Indian J Exp Biol 29:1095-1100.

Bi H, Sze CI (2002) N-methyl-D-aspartate receptor subunit NR2A and NR2B messenger RNA levels are altered in the hippocampus and entorhinal cortex in Alzheimer's disease. J Neurol Sci 200:11-18.

Biessels GJ, Kamal A, Ramakers GM, Urban IJ, Spruijt BM, Erkelens DW, Gispen WH (1996) Place learning and hippocampal synaptic plasticity in streptozotocin-induced diabetic rats. Diabetes 45:1259-1266.

Bitan G, Vollers SS, Teplow DB (2003) Elucidation of primary structure elements controlling early amyloid beta-protein oligomerization. J Biol Chem 278:34882-34889.

Blattner SM, Kretzler M (2005) Integrin-linked kinase in renal disease: connecting cell-matrix interaction to the cytoskeleton. Curr Opin Nephrol Hypertens 14:404-410.

Bliss T, Lomo T (1973a) Long-lasting potentiation of synaptic transmission in the dentate area of the anaesthetized rabbit following stimulation of the perforant path. J Physiol (Lond) 232:331 - 356.

Bliss TV, Lomo T (1973b) Long-lasting potentiation of synaptic transmission in the dentate area of the anaesthetized rabbit following stimulation of the perforant path. J Physiol 232:331-356.

Bliss TV, Collingridge GL (1993) A synaptic model of memory: long-term potentiation in the hippocampus. Nature 361:31-39.

Bliss TV, Collingridge GL, Morris RG (2003) Introduction. Long-term potentiation and structure of the issue. Philos Trans R Soc Lond B Biol Sci 358:607-611.

Blokland A, Jolles J (1994) Behavioral and biochemical effects of an ICV injection of streptozotocin in old Lewis rats. Pharmacol Biochem Behav 47:833-837.

Blondel O, Portha B (1989) Early appearance of in vivo insulin resistance in adult streptozotocin-injected rats. Diabete Metab 15:382-387.

Blondel O, Bailbe D, Portha B (1989a) Relation of insulin deficiency to impaired insulin action in NIDDM adult rats given streptozocin as neonates. Diabetes 38:610-617.

Blondel O, Bailbe D, Portha B (1989b) In vivo insulin resistance in streptozotocin-diabetic rats--evidence for reversal following oral vanadate treatment. Diabetologia 32:185-190.

Boehm J, Kang MG, Johnson RC, Esteban J, Huganir RL, Malinow R (2006) Synaptic incorporation of AMPA receptors during LTP is controlled by a PKC phosphorylation site on GluR1. Neuron 51:213-225.

Borchelt DR, Thinakaran G, Eckman CB, Lee MK, Davenport F, Ratovitsky T, Prada CM, Kim G, Seekins S, Yager D, Slunt HH, Wang R, Seeger M, Levey AI, Gandy SE, Copeland NG, Jenkins NA, Price DL, Younkin SG, Sisodia SS (1996) Familial Alzheimer's disease-linked presenilin 1 variants elevate Abeta1-42/1-40 ratio in vitro and in vivo. Neuron 17:1005-1013.

Boyt AA, Taddei TK, Hallmayer J, Helmerhorst E, Gandy SE, Craft S, Martins RN (2000) The effect of insulin and glucose on the plasma concentration of Alzheimer's amyloid precursor protein. Neuroscience 95:727-734.

Brickley SG, Misra C, Mok MH, Mishina M, Cull-Candy SG (2003) NR2B and NR2D subunits coassemble in cerebellar Golgi cells to form a distinct NMDA receptor subtype restricted to extrasynaptic sites. J Neurosci 23:4958-4966.

Brookmeyer R, Gray S, Kawas C (1998) Projections of Alzheimer's disease in the United States and the public health impact of delaying disease onset. Am J Public Health 88:1337-1342.

Burnashev N, Monyer H, Seeburg PH, Sakmann B (1992) Divalent ion permeability of AMPA receptor channels is dominated by the edited form of a single subunit. Neuron 8:189-198.

Carmignoto G, Vicini S (1992) Activity-dependent decrease in NMDA receptor responses during development of the visual cortex. Science 258:1007-1011.

Castillo PE, Malenka RC, Nicoll RA (1997) Kainate receptors mediate a slow postsynaptic current in hippocampal CA3 neurons. Nature 388:182-186.

Chapman PF, White GL, Jones MW, Cooper-Blacketer D, Marshall VJ, Irizarry M, Younkin L, Good MA, Bliss TV, Hyman BT, Younkin SG, Hsiao KK (1999) Impaired synaptic plasticity and learning in aged amyloid precursor protein transgenic mice. Nat Neurosci 2:271-276.

Chen L, Chetkovich DM, Petralia RS, Sweeney NT, Kawasaki Y, Wenthold RJ, Bredt DS, Nicoll RA (2000) Stargazin regulates synaptic targeting of AMPA receptors by two distinct mechanisms. Nature 408:936-943.

Clark BA, Cull-Candy SG (2002) Activity-dependent recruitment of extrasynaptic NMDA receptor activation at an AMPA receptor-only synapse. J Neurosci 22:4428-4436.

Cole GM, Frautschy SA (2007) The role of insulin and neurotrophic factor signaling in brain aging and Alzheimer's Disease. Exp Gerontol 42:10-21.

Coronado R, Latorre R (1983) Phospholipid bilayers made from monolayers on patch-clamp pipettes. Biophys J 43:231-236.

Cossart R, Esclapez M, Hirsch JC, Bernard C, Ben-Ari Y (1998) GluR5 kainate receptor activation in interneurons increases tonic inhibition of pyramidal cells. Nat Neurosci 1:470-478.

Cossart R, Epsztein J, Tyzio R, Becq H, Hirsch J, Ben-Ari Y, Crepel V (2002) Quantal release of glutamate generates pure kainate and mixed AMPA/kainate EPSCs in hippocampal neurons. Neuron 35:147-159.

Costantini C, Scrable H, Puglielli L (2006) An aging pathway controls the TrkA to p75NTR receptor switch and amyloid beta-peptide generation. Embo J 25:1997-2006.

Cowie CC, Rust KF, Byrd-Holt DD, Eberhardt MS, Flegal KM, Engelgau MM, Saydah SH, Williams DE, Geiss LS, Gregg EW (2006) Prevalence of diabetes and impaired fasting glucose in adults in the U.S. population: National Health And Nutrition Examination Survey 1999-2002. Diabetes Care 29:1263-1268.

Craft S, Watson GS (2004) Insulin and neurodegenerative disease: shared and specific mechanisms. Lancet Neurol 3:169-178.

Cross DA, Alessi DR, Cohen P, Andjelkovich M, Hemmings BA (1995) Inhibition of glycogen synthase kinase-3 by insulin mediated by protein kinase B. Nature 378:785-789.

Crunelli V, Mayer ML (1984) Mg2+ dependence of membrane resistance increases evoked by NMDA in hippocampal neurones. Brain Res 311:392-396.

Dan Y, Poo MM (2004) Spike timing-dependent plasticity of neural circuits. Neuron 44:23-30.

Das P, Parsons AD, Scarborough J, Hoffman J, Wilson J, Thompson RN, Overton JM, Fadool DA (2005) Electrophysiological and behavioral phenotype of insulin receptor defective mice. Physiol Behav 86:287-296.

de la Monte SM, Tong M, Lester-Coll N, Plater M, Jr., Wands JR (2006) Therapeutic rescue of neurodegeneration in experimental type 3 diabetes: relevance to Alzheimer's disease. J Alzheimers Dis 10:89-109.

De Strooper B, Annaert W (2000) Proteolytic processing and cell biological functions of the amyloid precursor protein. J Cell Sci 113 (Pt 11):1857-1870.

Derkach V, Barria A, Soderling TR (1999) Ca2+/calmodulin-kinase II enhances channel conductance of alpha-amino-3-hydroxy-5-methyl-4-isoxazolepropionate type glutamate receptors. Proc Natl Acad Sci U S A 96:3269-3274.

Dingledine R, Borges K, Bowie D, Traynelis SF (1999) The glutamate receptor ion channels. Pharmacol Rev 51:7-61.

Dore S, Kar S, Quirion R (1997) Insulin-like growth factor I protects and rescues hippocampal neurons against beta-amyloid- and human amylin-induced toxicity. Proc Natl Acad Sci U S A 94:4772-4777.

Dore S, Bastianetto S, Kar S, Quirion R (1999) Protective and rescuing abilities of IGF-I and some putative free radical scavengers against beta-amyloid-inducing toxicity in neurons. Ann N Y Acad Sci 890:356-364.

Duelli R, Schrock H, Kuschinsky W, Hoyer S (1994) Intracerebroventricular injection of streptozotocin induces discrete local changes in cerebral glucose utilization in rats. Int J Dev Neurosci 12:737-743.

Dunah AW, Luo J, Wang YH, Yasuda RP, Wolfe BB (1998) Subunit composition of N-methyl-D-aspartate receptors in the central nervous system that contain the NR2D subunit. Mol Pharmacol 53:429-437.

Engert F, Bonhoeffer T (1999) Dendritic spine changes associated with hippocampal long-term synaptic plasticity. Nature 399:66-70.

Esteban JA, Shi SH, Wilson C, Nuriya M, Huganir RL, Malinow R (2003) PKA phosphorylation of AMPA receptor subunits controls synaptic trafficking underlying plasticity. Nat Neurosci 6:136-143.

Figlewicz DP, Szot P (1991) Insulin stimulates membrane phospholipid metabolism by enhancing endogenous alpha 1-adrenergic activity in the rat hippocampus. Brain Res 550:101-107.

Forrest D, Yuzaki M, Soares HD, Ng L, Luk DC, Sheng M, Stewart CL, Morgan JI, Connor JA, Curran T (1994) Targeted disruption of NMDA receptor 1 gene abolishes NMDA response and results in neonatal death. Neuron 13:325-338.

Frame S, Cohen P (2001) GSK3 takes centre stage more than 20 years after its discovery. Biochem J 359:1-16.

Frolich L, Blum-Degen D, Riederer P, Hoyer S (1999) A disturbance in the neuronal insulin receptor signal transduction in sporadic Alzheimer's disease. Ann N Y Acad Sci 893:290-293.

Fukazawa Y, Saitoh Y, Ozawa F, Ohta Y, Mizuno K, Inokuchi K (2003) Hippocampal LTP is accompanied by enhanced F-actin content within the dendritic spine that is essential for late LTP maintenance in vivo. Neuron 38:447-460.

Gardoni F, Kamal A, Bellone C, Biessels GJ, Ramakers GM, Cattabeni F, Gispent WH, Di Luca M (2002) Effects of streptozotocin-diabetes on the hippocampal NMDA receptor complex in rats. J Neurochem 80:438-447.

Gerges NZ, Backos DS, Rupasinghe CN, Spaller MR, Esteban JA (2006) Dual role of the exocyst in AMPA receptor targeting and insertion into the postsynaptic membrane. Embo J 25:1623-1634.

Gerozissis K (2003) Brain insulin: regulation, mechanisms of action and functions. Cell Mol Neurobiol 23:1-25.

Gispen WH, Biessels GJ (2000) Cognition and synaptic plasticity in diabetes mellitus. Trends Neurosci 23:542-549.

Goate A, Chartier-Harlin MC, Mullan M, Brown J, Crawford F, Fidani L, Giuffra L, Haynes A, Irving N, James L, et al. (1991) Segregation of a missense mutation in the amyloid precursor protein gene with familial Alzheimer's disease. Nature 349:704-706.

Goedert M, Crowther RA, Garner CC (1991) Molecular characterization of microtubule-associated proteins tau and MAP2. Trends Neurosci 14:193-199.

Goedert M, Spillantini MG, Jakes R, Rutherford D, Crowther RA (1989a) Multiple isoforms of human microtubule-associated protein tau: sequences and localization in neurofibrillary tangles of Alzheimer's disease. Neuron 3:519-526.

Goedert M, Spillantini MG, Potier MC, Ulrich J, Crowther RA (1989b) Cloning and sequencing of the cDNA encoding an isoform of microtubule-associated protein tau containing four tandem repeats: differential expression of tau protein mRNAs in human brain. Embo J 8:393-399.

Grimes CA, Jope RS (2001) The multifaceted roles of glycogen synthase kinase 3beta in cellular signaling. Prog Neurobiol 65:391-426.

Groc L, Heine M, Cousins SL, Stephenson FA, Lounis B, Cognet L, Choquet D (2006) NMDA receptor surface mobility depends on NR2A-2B subunits. Proc Natl Acad Sci U S A 103:18769-18774.

Grunblatt E, Hoyer S, Riederer P (2004) Gene expression profile in streptozotocin rat model for sporadic Alzheimer's disease. J Neural Transm 111:367-386.

Grunblatt E, Koutsilieri E, Hoyer S, Riederer P (2006) Gene expression alterations in brain areas of intracerebroventricular streptozotocin treated rat. J Alzheimers Dis 9:261-271.

Grunblatt E, Salkovic-Petrisic M, Osmanovic J, Riederer P, Hoyer S (2007) Brain insulin system dysfunction in streptozotocin intracerebroventricularly treated rats generates hyperphosphorylated tau protein. J Neurochem 101:757-770.

Grundke-Iqbal I, Iqbal K, Tung YC, Quinlan M, Wisniewski HM, Binder LI (1986a) Abnormal phosphorylation of the microtubule-associated protein tau (tau) in Alzheimer cytoskeletal pathology. Proc Natl Acad Sci U S A 83:4913-4917.

Grundke-Iqbal I, Iqbal K, Quinlan M, Tung YC, Zaidi MS, Wisniewski HM (1986b) Microtubule-associated protein tau. A component of Alzheimer paired helical filaments. J Biol Chem 261:6084-6089.

Guo S, Kim WJ, Lok J, Lee SR, Besancon E, Luo BH, Stins MF, Wang X, Dedhar S, Lo EH (2008) Neuroprotection via matrix-trophic coupling between cerebral endothelial cells and neurons. Proc Natl Acad Sci U S A 105:7582-7587.

Guo W, Jiang H, Gray V, Dedhar S, Rao Y (2007) Role of the integrin-linked kinase (ILK) in determining neuronal polarity. Dev Biol 306:457-468.

Haleem K, Lippa CF, Smith TW, Kowa H, Wu J, Iwatsubo T (2007) Presenilin-1 C410Y Alzheimer disease plaques contain synaptic proteins. Am J Alzheimers Dis Other Demen 22:137-144.

Hallschmid M, Benedict C, Born J, Kern W (2007) Targeting metabolic and cognitive pathways of the CNS by intranasal insulin administration. Expert Opin Drug Deliv 4:319-322.

Hanger DP, Hughes K, Woodgett JR, Brion JP, Anderton BH (1992) Glycogen synthase kinase-3 induces Alzheimer's disease-like phosphorylation of tau: generation of paired helical filament epitopes and neuronal localisation of the kinase. Neurosci Lett 147:58-62.

Hannigan GE, Leung-Hagesteijn C, Fitz-Gibbon L, Coppolino MG, Radeva G, Filmus J, Bell JC, Dedhar S (1996) Regulation of cell adhesion and anchorage-dependent growth by a new beta 1-integrin-linked protein kinase. Nature 379:91-96.

Hashimoto K, Fukaya M, Qiao X, Sakimura K, Watanabe M, Kano M (1999) Impairment of AMPA receptor function in cerebellar granule cells of ataxic mutant mouse stargazer. J Neurosci 19:6027-6036.

Hayashi T, Huganir RL (2004) Tyrosine phosphorylation and regulation of the AMPA receptor by SRC family tyrosine kinases. J Neurosci 24:6152-6160.

Hayashi Y, Shi SH, Esteban JA, Piccini A, Poncer JC, Malinow R (2000) Driving AMPA receptors into synapses by LTP and CaMKII: requirement for GluR1 and PDZ domain interaction. Science 287:2262-2267.

Hebb DO (1949) The organization of behavior; a neuropsychological theory. New York,: Wiley.

Hebert LE, Scherr PA, Bienias JL, Bennett DA, Evans DA (2003) Alzheimer disease in the US population: prevalence estimates using the 2000 census. Arch Neurol 60:1119-1122.

Helzner EP, Scarmeas N, Cosentino S, Tang MX, Schupf N, Stern Y (2008) Survival in Alzheimer disease: a multiethnic, population-based study of incident cases. Neurology 71:1489-1495.

Hollmann M, Hartley M, Heinemann S (1991) Ca2+ permeability of KA-AMPA--gated glutamate receptor channels depends on subunit composition. Science 252:851-853.

Hollmann M, O'Shea-Greenfield A, Rogers SW, Heinemann S (1989) Cloning by functional expression of a member of the glutamate receptor family. Nature 342:643-648.

Hooper C, Markevich V, Plattner F, Killick R, Schofield E, Engel T, Hernandez F, Anderton B, Rosenblum K, Bliss T, Cooke SF, Avila J, Lucas JJ, Giese KP, Stephenson J, Lovestone S (2007) Glycogen synthase kinase-3 inhibition is integral to long-term potentiation. Eur J Neurosci 25:81-86.

Hoyer S (1996) Oxidative metabolism deficiencies in brains of patients with Alzheimer's disease. Acta Neurol Scand Suppl 165:18-24.

Hoyer S (2004) Glucose metabolism and insulin receptor signal transduction in Alzheimer disease. Eur J Pharmacol 490:115-125.

Hoyer S, Muller D, Plaschke K (1994) Desensitization of brain insulin receptor. Effect on glucose/energy and related metabolism. J Neural Transm Suppl 44:259-268.

Hume RI, Dingledine R, Heinemann SF (1991) Identification of a site in glutamate receptor subunits that controls calcium permeability. Science 253:1028-1031.

Impey S, Obrietan K, Storm DR (1999) Making new connections: role of ERK/MAP kinase signaling in neuronal plasticity. Neuron 23:11-14.

Iqbal K, Grundke-Iqbal I, Zaidi T, Merz PA, Wen GY, Shaikh SS, Wisniewski HM, Alafuzoff I, Winblad B (1986) Defective brain microtubule assembly in Alzheimer's disease. Lancet 2:421-426.

Ishii K, Ii K, Hasegawa T, Shoji S, Doi A, Mori H (1997) Increased A beta 42(43)-plaque deposition in early-onset familial Alzheimer's disease brains with the deletion of exon 9 and the missense point mutation (H163R) in the PS-1 gene. Neurosci Lett 228:17-20.

Iwashita A, Muramatsu Y, Yamazaki T, Muramoto M, Kita Y, Yamazaki S, Mihara K, Moriguchi A, Matsuoka N (2006) Neuroprotective Efficacy of Peroxisome Proliferator-Activated Receptor delta (PPAR-{delta}) Selective Agonists, L-165041 and GW501516, in Vitro and in Vivo. J Pharmacol Exp Ther.

Jacobsen JS, Wu CC, Redwine JM, Comery TA, Arias R, Bowlby M, Martone R, Morrison JH, Pangalos MN, Reinhart PH, Bloom FE (2006) Early-onset behavioral and synaptic deficits in a mouse model of Alzheimer's disease. Proc Natl Acad Sci U S A 103:5161-5166.

Jafferali S, Dumont Y, Sotty F, Robitaille Y, Quirion R, Kar S (2000) Insulin-like growth factor-I and its receptor in the frontal cortex, hippocampus, and cerebellum of normal human and alzheimer disease brains. Synapse 38:450-459.

Janson J, Laedtke T, Parisi JE, O'Brien P, Petersen RC, Butler PC (2004) Increased risk of type 2 diabetes in Alzheimer disease. Diabetes 53:474-481.

Jarrett JT, Lansbury PT, Jr. (1993) Seeding "one-dimensional crystallization" of amyloid: a pathogenic mechanism in Alzheimer's disease and scrapie? Cell 73:1055-1058.

Jarrett JT, Berger EP, Lansbury PT, Jr. (1993a) The carboxy terminus of the beta amyloid protein is critical for the seeding of amyloid formation: implications for the pathogenesis of Alzheimer's disease. Biochemistry 32:4693-4697.

Jarrett JT, Berger EP, Lansbury PT, Jr. (1993b) The C-terminus of the beta protein is critical in amyloidogenesis. Ann N Y Acad Sci 695:144-148.

Jiang H, Guo W, Liang X, Rao Y (2005) Both the establishment and the maintenance of neuronal polarity require active mechanisms: critical roles of GSK-3beta and its upstream regulators. Cell 120:123-135.

Jimenez Del Rio M, Velez-Pardo C (2006) Insulin-like growth factor-1 prevents Abeta[25-35]/(H2O2)- induced apoptosis in lymphocytes by reciprocal NF-kappaB activation and p53 inhibition via PI3K-dependent pathway. Growth Factors 24:67-78.

Johnson MW, Chotiner JK, Watson JB (1997) Isolation and characterization of synaptoneurosomes from single rat hippocampal slices. J Neurosci Methods 77:151-156.

Johnson-Farley NN, Patel K, Kim D, Cowen DS (2007) Interaction of FGF-2 with IGF-1 and BDNF in stimulating Akt, ERK, and neuronal survival in hippocampal cultures. Brain Res 1154:40-49.

Johnston AM, Pirola L, Van Obberghen E (2003) Molecular mechanisms of insulin receptor substrate protein-mediated modulation of insulin signalling. FEBS Lett 546:32-36.

Jonas P (2000) The Time Course of Signaling at Central Glutamatergic Synapses. News Physiol Sci 15:83-89.

Jonas P, Burnashev N (1995) Molecular mechanisms controlling calcium entry through AMPA-type glutamate receptor channels. Neuron 15:987-990.

Kaiyala KJ, Prigeon RL, Kahn SE, Woods SC, Schwartz MW (2000) Obesity induced by a high-fat diet is associated with reduced brain insulin transport in dogs. Diabetes 49:1525-1533.

Kamal A, Biessels GJ, Ramakers GM, Hendrik Gispen W (2005) The effect of short duration streptozotocin-induced diabetes mellitus on the late phase and threshold of long-term potentiation induction in the rat. Brain Res 1053:126-130.

Kang H, Welcher AA, Shelton D, Schuman EM (1997) Neurotrophins and time: different roles for TrkB signaling in hippocampal long-term potentiation. Neuron 19:653-664.

Kang J, Lemaire HG, Unterbeck A, Salbaum JM, Masters CL, Grzeschik KH, Multhaup G, Beyreuther K, Muller-Hill B (1987) The precursor of Alzheimer's disease amyloid A4 protein resembles a cell-surface receptor. Nature 325:733-736.

Katz B, Miledi R (1973) The binding of acetylcholine to receptors and its removal from the synaptic cleft. J Physiol 231:549-574.

Kern W, Born J, Schreiber H, Fehm HL (1999) Central nervous system effects of intranasally administered insulin during euglycemia in men. Diabetes 48:557-563.

Kew JN, Richards JG, Mutel V, Kemp JA (1998) Developmental changes in NMDA receptor glycine affinity and ifenprodil sensitivity reveal three distinct populations of NMDA receptors in individual rat cortical neurons. J Neurosci 18:1935-1943.

Khan TK, Alkon DL (2006) An internally controlled peripheral biomarker for Alzheimer's disease: Erk1 and Erk2 responses to the inflammatory signal bradykinin. Proc Natl Acad Sci U S A 103:13203-13207.

Khazipov R, Congar P, Ben-Ari Y (1995) Hippocampal CA1 lacunosum-moleculare interneurons: comparison of effects of anoxia on excitatory and inhibitory postsynaptic currents. J Neurophysiol 74:2138-2149.

Kim CH, Lisman JE (1999) A role of actin filament in synaptic transmission and long-term potentiation. J Neurosci 19:4314-4324.

Kim SJ, Han Y (2005) Insulin inhibits AMPA-induced neuronal damage via stimulation of protein kinase B (Akt). J Neural Transm 112:179-191.

Kirschenbaum F, Hsu SC, Cordell B, McCarthy JV (2001) Glycogen synthase kinase-3beta regulates presenilin 1 C-terminal fragment levels. J Biol Chem 276:30701-30707.

Konrad RJ, Kudlow JE (2002) The role of O-linked protein glycosylation in beta-cell dysfunction. Int J Mol Med 10:535-539.

Konrad RJ, Zhang F, Hale JE, Knierman MD, Becker GW, Kudlow JE (2002) Alloxan is an inhibitor of the enzyme O-linked N-acetylglucosamine transferase. Biochem Biophys Res Commun 293:207-212.

Kozlovsky N, Belmaker RH, Agam G (2002) GSK-3 and the neurodevelopmental hypothesis of schizophrenia. Eur Neuropsychopharmacol 12:13-25.

Krucker T, Siggins GR, Halpain S (2000) Dynamic actin filaments are required for stable long-term potentiation (LTP) in area CA1 of the hippocampus. Proc Natl Acad Sci U S A 97:6856-6861.

Kulstad JJ, Green PS, Cook DG, Watson GS, Reger MA, Baker LD, Plymate SR, Asthana S, Rhoads K, Mehta PD, Craft S (2006) Differential modulation of plasma beta-amyloid by insulin in patients with Alzheimer disease. Neurology 66:1506-1510.

Lannert H, Hoyer S (1998) Intracerebroventricular administration of streptozotocin causes long-term diminutions in learning and memory abilities and in cerebral energy metabolism in adult rats. Behav Neurosci 112:1199-1208.

Larson J, Lynch G, Games D, Seubert P (1999) Alterations in synaptic transmission and long-term potentiation in hippocampal slices from young and aged PDAPP mice. Brain Res 840:23-35.

Lee HK, Takamiya K, Han JS, Man H, Kim CH, Rumbaugh G, Yu S, Ding L, He C, Petralia RS, Wenthold RJ, Gallagher M, Huganir RL (2003) Phosphorylation of the AMPA receptor GluR1 subunit is required for synaptic plasticity and retention of spatial memory. Cell 112:631-643.

Leibson CL, Rocca WA, Hanson VA, Cha R, Kokmen E, O'Brien PC, Palumbo PJ (1997) The risk of dementia among persons with diabetes mellitus: a population-based cohort study. Ann N Y Acad Sci 826:422-427.

Lester-Coll N, Rivera EJ, Soscia SJ, Doiron K, Wands JR, de la Monte SM (2006) Intracerebral streptozotocin model of type 3 diabetes: relevance to sporadic Alzheimer's disease. J Alzheimers Dis 9:13-33.

Levy-Lahad E, Wijsman EM, Nemens E, Anderson L, Goddard KA, Weber JL, Bird TD, Schellenberg GD (1995) A familial Alzheimer's disease locus on chromosome 1. Science 269:970-973.

Li B, Otsu Y, Murphy TH, Raymond LA (2003) Developmental decrease in NMDA receptor desensitization associated with shift to synapse and interaction with postsynaptic density-95. J Neurosci 23:11244-11254.

Li B, Chen N, Luo T, Otsu Y, Murphy TH, Raymond LA (2002) Differential regulation of synaptic and extra-synaptic NMDA receptors. Nat Neurosci 5:833-834.

Lim IA, Merrill MA, Chen Y, Hell JW (2003) Disruption of the NMDA receptor-PSD-95 interaction in hippocampal neurons with no obvious physiological short-term effect. Neuropharmacology 45:738-754.

Lin JW, Ju W, Foster K, Lee SH, Ahmadian G, Wyszynski M, Wang YT, Sheng M (2000) Distinct molecular mechanisms and divergent endocytotic pathways of AMPA receptor internalization. Nat Neurosci 3:1282-1290.

111

Liu XB, Murray KD, Jones EG (2004) Switching of NMDA receptor 2A and 2B subunits at thalamic and cortical synapses during early postnatal development. J Neurosci 24:8885-8895.

Luchsinger JA, Tang MX, Shea S, Mayeux R (2004) Hyperinsulinemia and risk of Alzheimer disease. Neurology 63:1187-1192.

Luo J, Wang Y, Yasuda RP, Dunah AW, Wolfe BB (1997) The majority of N-methyl-D-aspartate receptor complexes in adult rat cerebral cortex contain at least three different subunits (NR1/NR2A/NR2B). Mol Pharmacol 51:79-86.

Lynch MA (2004) Long-term potentiation and memory. Physiol Rev 84:87-136.

Magleby KL, Stevens CF (1972) The effect of voltage on the time course of end-plate currents. J Physiol 223:151-171.

Mai L, Jope RS, Li X (2002) BDNF-mediated signal transduction is modulated by GSK3beta and mood stabilizing agents. J Neurochem 82:75-83.

Malenka RC (1994) Synaptic plasticity in the hippocampus: LTP and LTD. Cell 78:535-538.

Malinow R, Malenka RC (2002) AMPA receptor trafficking and synaptic plasticity. Annu Rev Neurosci 25:103-126.

Markram H, Lubke J, Frotscher M, Sakmann B (1997) Regulation of synaptic efficacy by coincidence of postsynaptic APs and EPSPs. Science 275:213-215.

Martin SJ, Grimwood PD, Morris RG (2000) Synaptic plasticity and memory: an evaluation of the hypothesis. Annu Rev Neurosci 23:649-711.

Martin TM, Bandi N, Schulz R, Roberts C, Kompella UB (2002) Preparation of budesonide and budesonide-PLA microparticles using supercritical fluid precipitation technology. AAPS PharmSciTech 3.

Masters CL, Simms G, Weinman NA, Multhaup G, McDonald BL, Beyreuther K (1985) Amyloid plaque core protein in Alzheimer disease and Down syndrome. Proc Natl Acad Sci U S A 82:4245-4249.

Matus A (2000) Actin-based plasticity in dendritic spines. Science 290:754-758.

Mayer G, Nitsch R, Hoyer S (1990) Effects of changes in peripheral and cerebral glucose metabolism on locomotor activity, learning and memory in adult male rats. Brain Res 532:95-100.

Mayer ML, Westbrook GL, Guthrie PB (1984) Voltage-dependent block by Mg2+ of NMDA responses in spinal cord neurones. Nature 309:261-263.

Milstein AD, Nicoll RA (2008) Regulation of AMPA receptor gating and pharmacology by TARP auxiliary subunits. Trends Pharmacol Sci 29:333-339.

Milstein AD, Zhou W, Karimzadegan S, Bredt DS, Nicoll RA (2007) TARP subtypes differentially and dose-dependently control synaptic AMPA receptor gating. Neuron 55:905-918.

Misra C, Brickley SG, Farrant M, Cull-Candy SG (2000) Identification of subunits contributing to synaptic and extrasynaptic NMDA receptors in Golgi cells of the rat cerebellum. J Physiol 524 Pt 1:147-162.

Mohrmann R, Kohr G, Hatt H, Sprengel R, Gottmann K (2002) Deletion of the C-terminal domain of the NR2B subunit alters channel properties and synaptic targeting of N-methyl-D-aspartate receptors in nascent neocortical synapses. J Neurosci Res 68:265-275.

Monyer H, Sprengel R, Schoepfer R, Herb A, Higuchi M, Lomeli H, Burnashev N, Sakmann B, Seeburg PH (1992) Heteromeric NMDA receptors: molecular and functional distinction of subtypes. Science 256:1217-1221.

Morishima-Kawashima M, Hasegawa M, Takio K, Suzuki M, Yoshida H, Titani K, Ihara Y (1995) Proline-directed and non-proline-directed phosphorylation of PHF-tau. J Biol Chem 270:823-829.

Moriyoshi K, Masu M, Ishii T, Shigemoto R, Mizuno N, Nakanishi S (1991) Molecular cloning and characterization of the rat NMDA receptor. Nature 354:31-37.

Muller D, Lynch G (1988) Long-term potentiation differentially affects two components of synaptic responses in hippocampus. Proc Natl Acad Sci U S A 85:9346-9350.

Nakagawa T, Cheng Y, Ramm E, Sheng M, Walz T (2005) Structure and different conformational states of native AMPA receptor complexes. Nature 433:545-549.

113

Nakanishi S (1992) Molecular diversity of glutamate receptors and implications for brain function. Science 258:597-603.

Naska S, Park KJ, Hannigan GE, Dedhar S, Miller FD, Kaplan DR (2006) An essential role for the integrin-linked kinase-glycogen synthase kinase-3 beta pathway during dendrite initiation and growth. J Neurosci 26:13344-13356.

Neumann KF, Rojo L, Navarrete LP, Farias G, Reyes P, Maccioni RB (2008) Insulin resistance and Alzheimer's disease: molecular links & clinical implications. Curr Alzheimer Res 5:438-447.

Nishimune A, Isaac JT, Molnar E, Noel J, Nash SR, Tagaya M, Collingridge GL, Nakanishi S, Henley JM (1998) NSF binding to GluR2 regulates synaptic transmission. Neuron 21:87-97.

Nitsch R, Hoyer S (1991) Local action of the diabetogenic drug, streptozotocin, on glucose and energy metabolism in rat brain cortex. Neurosci Lett 128:199-202.

Nowak L, Bregestovski P, Ascher P, Herbet A, Prochiantz A (1984) Magnesium gates glutamate-activated channels in mouse central neurones. Nature 307:462-465.

Oliver WR, Jr., Shenk JL, Snaith MR, Russell CS, Plunket KD, Bodkin NL, Lewis MC, Winegar DA, Sznaidman ML, Lambert MH, Xu HE, Sternbach DD, Kliewer SA, Hansen BC, Willson TM (2001) A selective peroxisome proliferator-activated receptor delta agonist promotes reverse cholesterol transport. Proc Natl Acad Sci U S A 98:5306-5311.

Opazo P, Watabe AM, Grant SG, O'Dell TJ (2003) Phosphatidylinositol 3-kinase regulates the induction of long-term potentiation through extracellular signal-related kinase-independent mechanisms. J Neurosci 23:3679-3688.

Park CR, Seeley RJ, Craft S, Woods SC (2000) Intracerebroventricular insulin enhances memory in a passive-avoidance task. Physiol Behav 68:509-514.

Passafaro M, Piech V, Sheng M (2001) Subunit-specific temporal and spatial patterns of AMPA receptor exocytosis in hippocampal neurons. Nat Neurosci 4:917-926.

Pastalkova E, Serrano P, Pinkhasova D, Wallace E, Fenton AA, Sacktor TC (2006) Storage of spatial information by the maintenance mechanism of LTP. Science 313:1141-1144.

114

Pei JJ, Braak H, Gong CX, Grundke-Iqbal I, Iqbal K, Winblad B, Cowburn RF (2002a) Up-regulation of cell division cycle (cdc) 2 kinase in neurons with early stage Alzheimer's disease neurofibrillary degeneration. Acta Neuropathol 104:369-376.

Pei JJ, Braak H, An WL, Winblad B, Cowburn RF, Iqbal K, Grundke-Iqbal I (2002b) Up-regulation of mitogen-activated protein kinases ERK1/2 and MEK1/2 is associated with the progression of neurofibrillary degeneration in Alzheimer's disease. Brain Res Mol Brain Res 109:45-55.

Peineau S, Taghibiglou C, Bradley C, Wong TP, Liu L, Lu J, Lo E, Wu D, Saule E, Bouschet T, Matthews P, Isaac JT, Bortolotto ZA, Wang YT, Collingridge GL (2007) LTP inhibits LTD in the hippocampus via regulation of GSK3beta. Neuron 53:703-717.

Perlmuter LC, Hakami MK, Hodgson-Harrington C, Ginsberg J, Katz J, Singer DE, Nathan DM (1984) Decreased cognitive function in aging non-insulin-dependent diabetic patients. Am J Med 77:1043-1048.

Persidsky Y, Ramirez SH, Haorah J, Kanmogne GD (2006) Blood-brain barrier: structural components and function under physiologic and pathologic conditions. J Neuroimmune Pharmacol 1:223-236.

Petralia RS, Sans N, Wang YX, Wenthold RJ (2005) Ontogeny of postsynaptic density proteins at glutamatergic synapses. Mol Cell Neurosci 29:436-452.

Pfaffl MW (2001) A new mathematical model for relative quantification in real-time RT-PCR. Nucleic acids research 29:e45.

Planel E, Tatebayashi Y, Miyasaka T, Liu L, Wang L, Herman M, Yu WH, Luchsinger JA, Wadzinski B, Duff KE, Takashima A (2007) Insulin dysfunction induces in vivo tau hyperphosphorylation through distinct mechanisms. J Neurosci 27:13635-13648.

Planells-Cases R, Sun W, Ferrer-Montiel AV, Montal M (1993) Molecular cloning, functional expression, and pharmacological characterization of an N-methyl-D-aspartate receptor subunit from human brain. Proc Natl Acad Sci U S A 90:5057-5061.

Plaschke K, Hoyer S (1993) Action of the diabetogenic drug streptozotocin on glycolytic and glycogenolytic metabolism in adult rat brain cortex and hippocampus. Int J Dev Neurosci 11:477-483.

Platenik J, Kuramoto N, Yoneda Y (2000) Molecular mechanisms associated with long-term consolidation of the NMDA signals. Life Sci 67:335-364.

Plitzko D, Rumpel S, Gottmann K (2001) Insulin promotes functional induction of silent synapses in differentiating rat neocortical neurons. Eur J Neurosci 14:1412-1415.

Portha B, Blondel O, Serradas P, McEvoy R, Giroix MH, Kergoat M, Bailbe D (1989) The rat models of non-insulin dependent diabetes induced by neonatal streptozotocin. Diabete Metab 15:61-75.

Priel A, Kolleker A, Ayalon G, Gillor M, Osten P, Stern-Bach Y (2005) Stargazin reduces desensitization and slows deactivation of the AMPA-type glutamate receptors. J Neurosci 25:2682-2686.

Prybylowski K, Chang K, Sans N, Kan L, Vicini S, Wenthold RJ (2005) The synaptic localization of NR2B-containing NMDA receptors is controlled by interactions with PDZ proteins and AP-2. Neuron 47:845-857.

Rivera EJ, Goldin A, Fulmer N, Tavares R, Wands JR, de la Monte SM (2005) Insulin and insulin-like growth factor expression and function deteriorate with progression of Alzheimer's disease: link to brain reductions in acetylcholine. J Alzheimers Dis 8:247-268.

Roche KW, O'Brien RJ, Mammen AL, Bernhardt J, Huganir RL (1996) Characterization of multiple phosphorylation sites on the AMPA receptor GluR1 subunit. Neuron 16:1179-1188.

Rogaev EI, Sherrington R, Rogaeva EA, Levesque G, Ikeda M, Liang Y, Chi H, Lin C, Holman K, Tsuda T, et al. (1995) Familial Alzheimer's disease in kindreds with missense mutations in a gene on chromosome 1 related to the Alzheimer's disease type 3 gene. Nature 376:775-778.

Roos MD, Xie W, Su K, Clark JA, Yang X, Chin E, Paterson AJ, Kudlow JE (1998) Streptozotocin, an analog of N-acetylglucosamine, blocks the removal of O-GlcNAc from intracellular proteins. Proc Assoc Am Physicians 110:422-432.

Rosenmund C, Stern-Bach Y, Stevens CF (1998) The tetrameric structure of a glutamate receptor channel. Science 280:1596-1599.

Salkovic-Petrisic M, Hoyer S (2007) Central insulin resistance as a trigger for sporadic Alzheimer-like pathology: an experimental approach. J Neural Transm Suppl:217-233.

Salkovic-Petrisic M, Tribl F, Schmidt M, Hoyer S, Riederer P (2006) Alzheimer-like changes in protein kinase B and glycogen synthase kinase-3 in rat frontal cortex and hippocampus after damage to the insulin signalling pathway. J Neurochem 96:1005-1015.

Saltiel AR, Kahn CR (2001) Insulin signalling and the regulation of glucose and lipid metabolism. Nature 414:799-806.

Schnell E, Sizemore M, Karimzadegan S, Chen L, Bredt DS, Nicoll RA (2002) Direct interactions between PSD-95 and stargazin control synaptic AMPA receptor number. Proc Natl Acad Sci U S A 99:13902-13907.

Scimemi A, Fine A, Kullmann DM, Rusakov DA (2004) NR2B-containing receptors mediate cross talk among hippocampal synapses. J Neurosci 24:4767-4777.

Scoville WB, Milner B (1957) Loss of recent memory after bilateral hippocampal lesions. J Neurol Neurosurg Psychiatry 20:11-21.

Seeburg PH (2002) A-to-I editing: new and old sites, functions and speculations. Neuron 35:17-20.

Selkoe DJ (2002) Alzheimer's disease is a synaptic failure. Science 298:789-791.

Selkoe DJ, Podlisny MB (2002) Deciphering the genetic basis of Alzheimer's disease. Annu Rev Genomics Hum Genet 3:67-99.

Selkoe DJ, Wolfe MS (2007) Presenilin: running with scissors in the membrane. Cell 131:215-221.

Sheng M, Lee SH (2001) AMPA receptor trafficking and the control of synaptic transmission. Cell 105:825-828.

Sheng M, Cummings J, Roldan LA, Jan YN, Jan LY (1994) Changing subunit composition of heteromeric NMDA receptors during development of rat cortex. Nature 368:144-147.

Sherrington R, Rogaev EI, Liang Y, Rogaeva EA, Levesque G, Ikeda M, Chi H, Lin C, Li G, Holman K, et al. (1995) Cloning of a gene bearing missense mutations in early-onset familial Alzheimer's disease. Nature 375:754-760.

Shi J, Aamodt SM, Constantine-Paton M (1997) Temporal correlations between functional and molecular changes in NMDA receptors and GABA neurotransmission in the superior colliculus. J Neurosci 17:6264-6276.

Simons M, de Strooper B, Multhaup G, Tienari PJ, Dotti CG, Beyreuther K (1996) Amyloidogenic processing of the human amyloid precursor protein in primary cultures of rat hippocampal neurons. J Neurosci 16:899-908.

Simpson IA, Vannucci SJ, Maher F (1994) Glucose transporters in mammalian brain. Biochem Soc Trans 22:671-675.

Sjostrom PJ, Nelson SB (2002) Spike timing, calcium signals and synaptic plasticity. Curr Opin Neurobiol 12:305-314.

Skeberdis VA, Lan J, Zheng X, Zukin RS, Bennett MV (2001) Insulin promotes rapid delivery of N-methyl-D- aspartate receptors to the cell surface by exocytosis. Proc Natl Acad Sci U S A 98:3561-3566.

Snyder SW, Ladror US, Wade WS, Wang GT, Barrett LW, Matayoshi ED, Huffaker HJ, Krafft GA, Holzman TF (1994) Amyloid-beta aggregation: selective inhibition of aggregation in mixtures of amyloid with different chain lengths. Biophys J 67:1216-1228.

Sommer B, Kohler M, Sprengel R, Seeburg PH (1991) RNA editing in brain controls a determinant of ion flow in glutamate-gated channels. Cell 67:11-19.

Sommer B, Keinanen K, Verdoorn TA, Wisden W, Burnashev N, Herb A, Kohler M, Takagi T, Sakmann B, Seeburg PH (1990) Flip and flop: a cell-specific functional switch in glutamate-operated channels of the CNS. Science 249:1580-1585.

Soto D, Coombs ID, Kelly L, Farrant M, Cull-Candy SG (2007) Stargazin attenuates intracellular polyamine block of calcium-permeable AMPA receptors. Nat Neurosci 10:1260-1267.

Sprengel R, Suchanek B, Amico C, Brusa R, Burnashev N, Rozov A, Hvalby O, Jensen V, Paulsen O, Andersen P, Kim JJ, Thompson RF, Sun W, Webster LC, Grant SG, Eilers J, Konnerth A, Li J, McNamara JO, Seeburg PH (1998) Importance of

the intracellular domain of NR2 subunits for NMDA receptor function in vivo. Cell 92:279-289.

Steen E, Terry BM, Rivera EJ, Cannon JL, Neely TR, Tavares R, Xu XJ, Wands JR, de la Monte SM (2005) Impaired insulin and insulin-like growth factor expression and signaling mechanisms in Alzheimer's disease--is this type 3 diabetes? J Alzheimers Dis 7:63-80.

Steigerwald F, Schulz TW, Schenker LT, Kennedy MB, Seeburg PH, Kohr G (2000) C-Terminal truncation of NR2A subunits impairs synaptic but not extrasynaptic localization of NMDA receptors. J Neurosci 20:4573-4581.

Steward O, Schuman EM (2003) Compartmentalized synthesis and degradation of proteins in neurons. Neuron 40:347-359.

Strandell E, Eizirik DL, Sandler S (1989) Survival and B-cell function of mouse pancreatic islets maintained in culture after concomitant exposure to streptozotocin and nicotinamide. Exp Clin Endocrinol 93:219-224.

Sui L, Wang J, Li BM (2008) Role of the phosphoinositide 3-kinase-Akt-mammalian target of the rapamycin signaling pathway in long-term potentiation and trace fear conditioning memory in rat medial prefrontal cortex. Learn Mem 15:762-776.

Takadera T, Sakura N, Mohri T, Hashimoto T (1993) Toxic effect of a beta-amyloid peptide (beta 22-35) on the hippocampal neuron and its prevention. Neurosci Lett 161:41-44.

Taniguchi CM, Emanuelli B, Kahn CR (2006) Critical nodes in signalling pathways: insights into insulin action. Nat Rev Mol Cell Biol 7:85-96.

Thomas CG, Miller AJ, Westbrook GL (2006) Synaptic and extrasynaptic NMDA receptor NR2 subunits in cultured hippocampal neurons. J Neurophysiol 95:1727-1734.

Tomita S, Adesnik H, Sekiguchi M, Zhang W, Wada K, Howe JR, Nicoll RA, Bredt DS (2005) Stargazin modulates AMPA receptor gating and trafficking by distinct domains. Nature 435:1052-1058.

Toni N, Buchs PA, Nikonenko I, Bron CR, Muller D (1999) LTP promotes formation of multiple spine synapses between a single axon terminal and a dendrite. Nature 402:421-425.

Tovar KR, Westbrook GL (1999) The incorporation of NMDA receptors with a distinct subunit composition at nascent hippocampal synapses in vitro. J Neurosci 19:4180-4188.

Tsien JZ, Huerta PT, Tonegawa S (1996) The essential role of hippocampal CA1 NMDA receptor-dependent synaptic plasticity in spatial memory. Cell 87:1327-1338.

Turetsky D, Garringer E, Patneau DK (2005) Stargazin modulates native AMPA receptor functional properties by two distinct mechanisms. J Neurosci 25:7438-7448.

Turrigiano GG, Leslie KR, Desai NS, Rutherford LC, Nelson SB (1998) Activity-dependent scaling of quantal amplitude in neocortical neurons. Nature 391:892-896.

U'Ren RC, Riddle MC, Lezak MD, Bennington-Davis M (1990) The mental efficiency of the elderly person with type II diabetes mellitus. J Am Geriatr Soc 38:505-510.

Vaithianathan T, Manivannan K, Kleene R, Bahr BA, Dey MP, Dityatev A, Suppiramaniam V (2005) Single channel recordings from synaptosomal AMPA receptors. Cell Biochem Biophys 42:75-85.

Valastro B, Cossette J, Lavoie N, Gagnon S, Trudeau F, Massicotte G (2002) Up-regulation of glutamate receptors is associated with LTP defects in the early stages of diabetes mellitus. Diabetologia 45:642-650.

Vandenberghe W, Nicoll RA, Bredt DS (2005) Stargazin is an AMPA receptor auxiliary subunit. Proc Natl Acad Sci U S A 102:485-490.

Vassar R (2004) BACE1: the beta-secretase enzyme in Alzheimer's disease. J Mol Neurosci 23:105-114.

Wagner N, Jehl-Pietri C, Lopez P, Murdaca J, Giordano C, Schwartz C, Gounon P, Hatem SN, Grimaldi P, Wagner KD (2009) Peroxisome proliferator-activated receptor {beta} stimulation induces rapid cardiac growth and angiogenesis via direct activation of calcineurin. Cardiovasc Res.

Walsh DM, Klyubin I, Fadeeva JV, Cullen WK, Anwyl R, Wolfe MS, Rowan MJ, Selkoe DJ (2002) Naturally secreted oligomers of amyloid beta protein potently inhibit hippocampal long-term potentiation in vivo. Nature 416:535-539.

Wan Q, Xiong ZG, Man HY, Ackerley CA, Braunton J, Lu WY, Becker LE, MacDonald JF, Wang YT (1997) Recruitment of functional GABA(A) receptors to postsynaptic domains by insulin. Nature 388:686-690.

Wang J, Dickson DW, Trojanowski JQ, Lee VM (1999) The levels of soluble versus insoluble brain Abeta distinguish Alzheimer's disease from normal and pathologic aging. Exp Neurol 158:328-337.

Wang JY, Gualco E, Peruzzi F, Sawaya BE, Passiatore G, Marcinkiewicz C, Staniszewska I, Ferrante P, Amini S, Khalili K, Reiss K (2007) Interaction between serine phosphorylated IRS-1 and beta1-integrin affects the stability of neuronal processes. J Neurosci Res 85:2360-2373.

Watson GS, Craft S (2003) The role of insulin resistance in the pathogenesis of Alzheimer's disease: implications for treatment. CNS Drugs 17:27-45.

Watson GS, Craft S (2004) Modulation of memory by insulin and glucose: neuropsychological observations in Alzheimer's disease. Eur J Pharmacol 490:97-113.

Werther GA, Hogg A, Oldfield BJ, McKinley MJ, Figdor R, Allen AM, Mendelsohn FA (1987) Localization and characterization of insulin receptors in rat brain and pituitary gland using in vitro autoradiography and computerized densitometry. Endocrinology 121:1562-1570.

West AE, Griffith EC, Greenberg ME (2002) Regulation of transcription factors by neuronal activity. Nat Rev Neurosci 3:921-931.

West AE, Chen WG, Dalva MB, Dolmetsch RE, Kornhauser JM, Shaywitz AJ, Takasu MA, Tao X, Greenberg ME (2001) Calcium regulation of neuronal gene expression. Proc Natl Acad Sci U S A 98:11024-11031.

Whitlock JR, Heynen AJ, Shuler MG, Bear MF (2006) Learning induces long-term potentiation in the hippocampus. Science 313:1093-1097.

Wisniewski T, Dowjat WK, Buxbaum JD, Khorkova O, Efthimiopoulos S, Kulczycki J, Lojkowska W, Wegiel J, Wisniewski HM, Frangione B (1998) A novel Polish presenilin-1 mutation (P117L) is associated with familial Alzheimer's disease and leads to death as early as the age of 28 years. Neuroreport 9:217-221.

Wu LG, Saggau P (1994) Presynaptic calcium is increased during normal synaptic transmission and paired-pulse facilitation, but not in long-term potentiation in area CA1 of hippocampus. J Neurosci 14:645-654.

Xia J, Zhang X, Staudinger J, Huganir RL (1999) Clustering of AMPA receptors by the synaptic PDZ domain-containing protein PICK1. Neuron 22:179-187.

Xie L, Helmerhorst E, Taddei K, Plewright B, Van Bronswijk W, Martins R (2002) Alzheimer's beta-amyloid peptides compete for insulin binding to the insulin receptor. J Neurosci 22:RC221.

Xing C, Yin Y, He X, Xie Z (2006) Effects of insulin-like growth factor 1 on voltage-gated ion channels in cultured rat hippocampal neurons. Brain Res 1072:30-35.

Xing C, Yin Y, Chang R, Gong X, He X, Xie Z (2007) Effects of insulin-like growth factor 1 on synaptic excitability in cultured rat hippocampal neurons. Exp Neurol 205:222-229.

Yang Y, Wang XB, Frerking M, Zhou Q (2008) Spine expansion and stabilization associated with long-term potentiation. J Neurosci 28:5740-5751.

Zhang J, Diamond JS (2006) Distinct perisynaptic and synaptic localization of NMDA and AMPA receptors on ganglion cells in rat retina. J Comp Neurol 498:810-820.

Zhao W, Chen H, Xu H, Moore E, Meiri N, Quon MJ, Alkon DL (1999) Brain insulin receptors and spatial memory. Correlated changes in gene expression, tyrosine phosphorylation, and signaling molecules in the hippocampus of water maze trained rats. J Biol Chem 274:34893-34902.

Zhao WQ, De Felice FG, Fernandez S, Chen H, Lambert MP, Quon MJ, Krafft GA, Klein WL (2008) Amyloid beta oligomers induce impairment of neuronal insulin receptors. Faseb J 22:246-260.

Zhou Q, Xiao M, Nicoll RA (2001) Contribution of cytoskeleton to the internalization of AMPA receptors. Proc Natl Acad Sci U S A 98:1261-1266.

Zhu JJ, Qin Y, Zhao M, Van Aelst L, Malinow R (2002) Ras and Rap control AMPA receptor trafficking during synaptic plasticity. Cell 110:443-455.

Zhu LQ, Wang SH, Liu D, Yin YY, Tian Q, Wang XC, Wang Q, Chen JG, Wang JZ (2007) Activation of glycogen synthase kinase-3 inhibits long-term potentiation with synapse-associated impairments. J Neurosci 27:12211-12220.